EC-Sense: Radio Energy Capture for Ultra-Low-Power Wireless Soil Moisture Sensing

YOGANAND BIRADAVOLU, University of Wisconsin–Madison, USA
JIAN DING, Yale University, USA
BHUVANA KRISHNASWAMY, University of Wisconsin–Madison, USA
LEANDROS TASSIULAS, Yale University, USA
VAISHNAVI RANGANATHAN, Microsoft Research, USA

Understanding spatial and temporal variations in soil moisture is critical for sustainable agriculture. Contactless approaches such as ground-penetrating radar and satellite sensing are either expensive or offer limited resolution, making them less scalable. In-situ sensors provide higher resolution but often involve challenging data retrieval processes and wired infrastructure. In this work, we propose EC-Sense, a wire-free system for in-situ soil moisture sensing that employs ultra-low-power sensor Tags buried underground and reference Tags placed on the surface. EC-Sense introduces a novel sensing modality based on energy capture time (EC Time), defined as the time taken by a sensor Tag to harvest sufficient energy to activate a response. EC Time serves as a proxy for path loss in soil, which correlates strongly with soil moisture. By leveraging differential path loss—estimated from the EC Times of both surface and buried Tags—EC-Sense isolates soil-induced attenuation from environmental effects above ground. This differential sensing approach, combined with a decoupled sensing and communication architecture, enables EC-Sense to overcome limitations of existing wideband RF-based sensors. Despite using an active radio, our Tags consume only 3.7 μW on average and achieve a projected lifetime of 10 years under realistic conditions. We deployed EC-Sense in an open agricultural field for over a week and measured soil moisture at multiple depths daily, achieving 98% accuracy compared to ground truth. We further evaluate EC-Sense across three representative soil types—sandy loam, silt loam, and silty clay loam—and demonstrate reliable sensing at depths of 40 cm, 30 cm, and 25 cm, respectively, at field capacity.

CCS Concepts: • **Computer systems organization → Embedded and cyber-physical systems**; • **Hardware → Energy harvesting**; **Communication hardware, interfaces and storage**; • **Applied computing → Agriculture**.

Additional Key Words and Phrases: Soil moisture sensing, Energy harvesting, Wireless sensing, Ultra-low-power

ACM Reference Format:
Yoganand Biradavolu, Jian Ding, Bhuvana Krishnaswamy, Leandros Tassiulas, and Vaishnavi Ranganathan. 2025. EC-Sense: Radio Energy Capture for Ultra-Low-Power Wireless Soil Moisture Sensing. *Proc. ACM Interact. Mob. Wearable Ubiquitous Technol.* 9, 4, Article 160 (December 2025), 27 pages. https://doi.org/10.1145/3770660

1 INTRODUCTION

Informed decision-making in irrigating large agricultural fields is essential not only for water conservation but, more importantly, to prevent crop stress from water-logging and nutrient leaching [15, 42]. Poor irrigation practices can wash away essential nutrients and contaminate water sources, posing environmental and health

Authors' Contact Information: Yoganand Biradavolu, University of Wisconsin–Madison, USA, ybiradavolu@wisc.edu; Jian Ding, Yale University, USA, jian.ding@yale.edu; Bhuvana Krishnaswamy, University of Wisconsin–Madison, USA, bhuvana@ece.wisc.edu; Leandros Tassiulas, Yale University, USA, leandros.tassiulas@yale.edu; Vaishnavi Ranganathan, Microsoft Research, USA, vnattar@microsoft.com.

This work is licensed under a Creative Commons Attribution-ShareAlike 4.0 International License.
© 2025 Copyright held by the owner/author(s).
ACM 2474-9567/2025/12-ART160
https://doi.org/10.1145/3770660

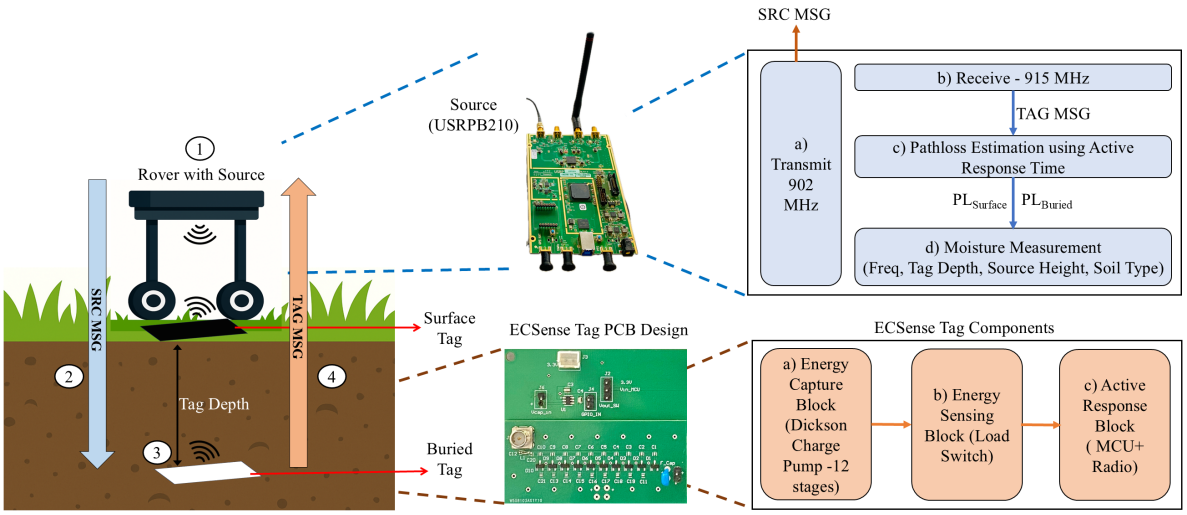

Fig. 1. EC-Sense Framework : ① Source transmits a tone (SRC-MSG)②a at 902MHz to power the Tag. Tags ③ on the surface and buried harvest energy using energy capture circuit ③a and input to the energy sensing block ③b which then triggers the active radio ③c to send the TAG-MSG. Source ① receives ①b at 915MHz; on detecting the Tag responses, calculates Active Response Time (ART) and path loss ①c for each Tag. Source measures soil moisture using ART (①d) with inputs such as Tag depth, Source height, soil type and signal frequency.

risks [5]. These challenges are amplified across large, heterogeneous fields with rapidly changing soil conditions, making it critical to monitor soil moisture with high spatial and temporal resolution [56, 65].

Today, the high installation and maintenance costs of in-situ sensors [30, 43] pose a challenge to capturing soil moisture heterogeneity in a field, often making it impractical or unaffordable for farmers. Even when sensors are affordable [18, 25, 40], data retrieval and the use of batteries that require frequent replacement increase the overall cost. Moreover, reliable sensing that is tolerant to environmental changes is essential for long-term deployability but is difficult to establish at the wide-area scale. Thus, to capture the spatial and temporal diversity of soil moisture in vast agricultural fields, we identify four key requirements for sensor design:

(1) In-situ measurements at multiple depths: In agricultural soil sensing, buried sensors are generally preferred for two key reasons—they are unobtrusive and they help understand water penetration at various depths below the surface [43, 83].
(2) Wire-free sensors to overcome the deployment challenges posed by wires in real-world settings, such as pests chewing on wires [12, 88].
(3) Ultra-low-power sensors to reduce the deployment and maintenance costs of replacing batteries. Wireless communication is often the sought-out solution for sensing systems, but it comes at the added cost of power. For battery-operated sensors, this limits their lifetime, especially when deployed at large scale [41, 45, 46].
(4) Sensors that are resilient to changes in weather and environmental conditions and are unaffected by agricultural processes in the field.

To meet these requirements, recent efforts have explored wireless and RF-based solutions that aim to eliminate wires, reduce power consumption, and enable buried deployments. While these approaches offer promising directions, each comes with its own limitations—be it in terms of sensing depth, power efficiency, or cost. Techniques based on commodity WiFi, LTE, or LoRa receivers extract phase or amplitude variations in the

received signals to infer moisture but typically require buried active receivers and wired infrastructure, limiting scalability [10, 20, 29, 87]. Moreover, phase-based techniques are highly sensitive to environmental changes—such as antenna displacement, temperature, or multipath—which degrade robustness and make soil moisture inference challenging [11, 19, 29, 53, 57]. Propagation-delay-based methods estimate moisture from the round-trip time (RTT) of radio signals, which correlates with soil permittivity. However, due to short underground distances, these delays are in the nanosecond range, requiring high bandwidths and precise clocks with frequent calibration, constraining practicality [21, 45]. Passive backscatter techniques modulate reflected signals to encode moisture-induced changes in the environment, enabling ultra-low-power operation. Yet, these methods suffer from dual path loss in soil—once when the signal reaches the tag and again on the return path—thereby limiting sensing depth and often requiring wide bandwidths [43, 86]. Table 1 summarizes these trade-offs across key system characteristics, and we note that there is a clear need for a soil moisture sensing system that satisfies all the requirements of being buried, low-power, wire-free, and resilient to environmental changes, as identified above.

Table 1. Comparison of RF-based soil moisture sensing systems.

Sensor	**Max Depth ≥ 40 cm**	**No Buried Wires**	**Battery Life ≥ 10 yrs**	**Bandwidth < 1GHz**
Strobe [20]	✗	✗	✗	✓
SMOL [47]	✗	✓	✗	✓
LTE-Soil-Meter [29]	✗	✗	✗	✓
CoMEt [45]	✗	✓	✓	✗
SoilId [21]	✗	✓	✓	✗
GreenTag [86]	✗	✓	✓	✓
SoilCares [87]	✓	✓	✗	✓
MetaSoil [12]	✓	✓	✓	✗
ECSense (This Work)	✓	✓	✓	✓

In this work, we propose EC-Sense (Energy Capture Sense), a new framework for measuring in-situ soil moisture by observing the differential time to capture radio signal energy between the surface and underground. EC-Sense decouples sensing and communication to overcome the challenges associated with conventional RTT- or phase-based RF sensing. Our sensor Tags use energy harvesting circuits to capture radio signals from an RF Source above ground. The time required to accumulate a threshold of energy—*Energy Capture time (EC time)*—is indicative of the incident RF power, which is directly affected by path loss in soil, soil type, moisture, frequency, and Tag depth. By deriving the path loss from EC time, and measuring the differential path loss between buried and reference surface Tags, we isolate the soil's contribution and accurately infer soil moisture. To the best of our knowledge, this is the first work to introduce EC time and establish a quantitative relationship between EC time and soil dielectric properties. Therefore, EC-Sense opens a new direction for low-power, scalable in-situ environmental monitoring.

EC-Sense, as illustrated in Figure 1, includes an RF Source above ground that transmits radio signals toward the sensor Tags—a reference surface Tag and other buried Tags at various depths underground. The reference Tags on the surface and the buried Tags simultaneously capture the radio signal energy; upon capturing a predefined threshold of energy, they each respond with a short message using an active radio. The time difference between the source excitation and the active response from the Tags is equal to the sum of propagation delays in air, soil (for the buried Tag), and the time to capture energy at the Tag. Since energy capture times are orders of magnitude higher than propagation delays at such short distances [52, 81], the measured time difference is approximately equal to the energy capture time (EC time) for a predetermined amount of energy. For a given energy capture

circuit, EC time is a strong indicator of the incident power at the Tag, making it a more reliable proxy for the path loss in soil. The use of EC time for path loss estimation decouples bandwidth from depth resolution; thus, the accuracy of delay estimation becomes solely a function of the harvesting circuit. To the best of our knowledge, this is the first approach that utilizes time for energy capture to estimate channel (soil) properties. Additionally, the use of surface Tags as a reference helps isolate the effect of soil from that of the surface environment in real time. This architecture eliminates the need to calibrate the EC-Sense framework, making it agnostic to changing environments around the deployment site.

We make the following contributions toward our goal of building wire-free, ultra-low-power buried Tags that are agnostic to environmental changes for capturing in-situ soil moisture.

- We propose EC-Sense, an in-situ soil moisture sensing framework built on a wire-free, buried, and ultra-low-power sensor architecture that is tolerant to environmental changes at the deployment site. EC-Sense uses a differential measurement method based on a buried Tag and a decoupled surface Tag. We discuss the design of the framework and its components in Sections 2 and 3.1.
- We present a novel approach to measuring path loss in soil through energy capture time (henceforth referred to as EC time). We measure EC time indirectly by observing the active response time of the buried Tag and estimating the radio path loss using the mathematical relationship between EC time and the incident RF power at the Tags. Section 9 provides the primer, and our model is presented in Section 3.2.
- We derive the path loss model of a radio signal propagating through soil and air, and then measure soil moisture using the differential path loss between buried and surface Tags and the derived model. The path loss estimation and differential sensing approach to isolate path loss in soil is detailed in Section 3.3.
- We design and prototype the ultra-low-power EC-Sense Tags*. Section 4 provides the design and prototyping details. We deployed EC-Sense in an open agricultural farm over the course of a week under varying weather conditions to characterize its performance.
- We evaluate EC-Sense across three different soil types—sandy loam, silt loam, and silty clay loam. Our results show that EC-Sense can measure soil moisture with approximately 98% accuracy compared to ground truth, achieving maximum sensing depths of 40 cm in sandy loam, 30 cm in silt loam, and 25 cm in silty clay loam at field capacity conditions (Section 5).

2 EC SENSE: SYSTEM OVERVIEW

This work aims to implement a novel, practical, ultra-low-power system that can measure moisture content at various depths in soil while being environment-agnostic and less obtrusive. We achieve this with the help of the EC-Sense architecture, which is built on decoupled surface and buried sensor Tags and a radio Source (transceiver) placed above ground. Figure 1 illustrates our proposed framework. EC-Sense consists of two ultra-low-power sensor Tags—one buried and one on the surface (black and white tiles; ③ in Fig. 1)—along with an RF Source (①), which broadcasts a continuous tone from above the surface oriented toward the Tags as shown (② – SRC-MSG). Both Tags capture energy from this tone; upon capturing a predefined threshold of energy, they turn on their respective active radios (③c) and respond with a pre-coded short message (④ – TAG-MSG). The EC time (time to capture energy) on these Tags is inversely proportional to the incident power on them. The incident power at the Tag is directly affected by the path loss experienced by the radio signal from the Source as it travels first through air, then through soil (SRC-MSG). Since path loss in soil is a function of soil type and moisture [20, 43, 86], there exists a clear mapping between EC time, path loss, and soil moisture. The buried Tag captures the path loss experienced in soil as well as above ground, whereas the surface Tag captures only the impact of the environment above ground. Thus, the differential path loss, obtained from the EC times measured by the surface and buried Tags, reflects the path loss experienced only in soil. The surface Tag helps isolate the impact of air and keeps

*https://anonymous.4open.science/r/ECSense-System/

EC-Sense agnostic to above-surface environmental conditions. To overcome the practical challenge of placing sensors on the surface and reduce deployment cost, we envision a drone or agricultural rover [3, 7] carrying the RF Source and the surface Tag. More details on this design are provided in Section 6.

In contrast to prior work built on backscatter-based tags [43, 86], EC-Sense Tags use an active radio to send their response. This design choice—favoring a low-power active radio—is intended to increase the maximum attainable depth by eliminating the dual path loss faced in backscatter communication. In EC-Sense, the TAG-MSG is sent using an active radio, where the buried sensing depth is a function of the signal strength and the distance from the Tag to the receiver, thus improving Tag depth. The active radio is turned on only when the captured energy exceeds a threshold, and hence consumes low power. A more detailed comparison with backscatter systems addressing the depth and power trade-off is provided in Section 5.7.

3 EC SENSE: SYSTEM DESIGN

Buried sensors are preferred for in-situ soil moisture sensing as they enable accurate measurements at various depths [20, 43, 45]. However, insights from soil scientists and practitioners highlight that reliance on wired sensors—and the frequent calibration they require to account for environmental variability—poses significant deployment challenges. *Therefore, wire-free, ultra-low-power, and resilient soil moisture sensing using buried sensors is desired for practical wide-acre sensing.*

As RF signals propagate through soil, they experience higher attenuation compared to air, with the rate of attenuation proportional to moisture content. Thus, path loss serves as a strong indicator of soil moisture for a given soil type. In this work, we propose measuring soil moisture by estimating the path loss encountered by an RF signal as it traverses through air and soil. Direct measurement of path loss in soil using radio signals is challenging; systems like Ground Penetrating Radar (GPR) require high transmit power, wideband spectrum, and extremely sensitive receivers, making them expensive. Indirect methods that use RF signals for moisture sensing face limitations in meeting the requirements of low-cost, low-power in-situ moisture sensing (Section 1).

We propose EC-Sense, a novel approach to measuring soil moisture using ultra-low-power Tags that decouples communication and path loss estimation. EC-Sense uses an RF Source to broadcast a continuous tone (SRC-MSG) and two Tags—one on the surface and one buried—each equipped with ultra-low-power active radios. The Tags capture energy from the RF signal and respond with a short (16-bit FSK) message (TAG-MSG) once they accumulate sufficient energy exceeding a predefined voltage threshold (V_{Thresh}). We estimate the incident RF power at each Tag by calculating the active response time (ART), defined as the time difference between transmitting the SRC-MSG and receiving the TAG-MSG at the Source. Since the propagation delay at these distances (<1m) is negligible (on the order of nanoseconds) compared to the EC time (on the order of milliseconds to seconds), ART is dominated by EC time. Higher soil moisture results in greater path loss, leading to lower incident power, longer EC time, and hence a longer ART. Setting a fixed V_{Thresh} allows consistent estimation of EC time, which reflects the incident RF power and varies with soil moisture conditions. By comparing path loss measurements from the surface Tag (air-only path loss) and the buried Tag (air + soil path loss), we effectively cancel out the effect of the surface and isolate the contribution of soil moisture. This enables EC-Sense to achieve robust, scalable, and ultra-low-power soil moisture sensing. Towards building EC-Sense, we identify and address the following three key challenges:

- Designing an ultra-low-power Tag that can trigger a radio response upon capturing energy, indicating that the voltage on the capacitor has exceeded V_{Thresh} (§3.1).
- Estimating RF incident power at the Tags—and in turn, path loss in soil—accurately from ART (§3.2).
- Determining the soil moisture from the incident power and path loss estimates using the two Tags (§3.3).

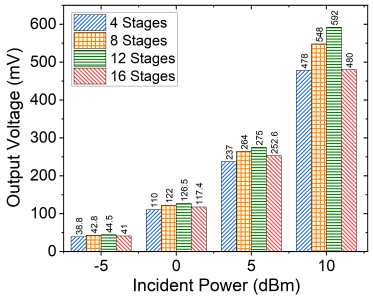

Fig. 2. EC voltage at increasing incident powers. Voltage amplification saturates at 12 stages.

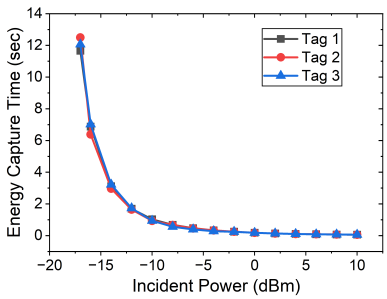

Fig. 3. Wired evaluations showing consistency in measured EC time across tags

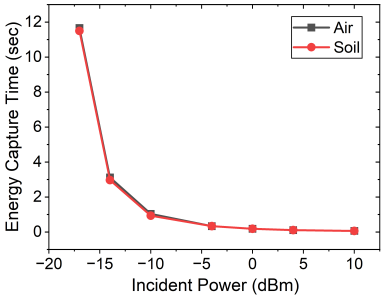

Fig. 4. Evaluation to demonstrate consistent EC time vs.incident power with tag in air vs. soil.

3.1 EC-Sense Tag Design

EC-Sense Tags capture energy from the RF Source located above ground. The Tags are designed to sense the voltage generated by the energy capture circuit (EC voltage), and when this voltage exceeds a predefined threshold (V_{Thresh}), the active radio transmits a short message back. A EC-Sense Tag consists of three blocks responsible for: (1) energy capture, (2) energy sensing, and (3) active response, as shown in Figure 1.

Energy Capture (EC) Block: The EC block converts incident RF energy into usable DC voltage using a half-wave rectifier followed by a voltage multiplication stage. We adapt from established RF energy harvesting designs for sensing [69, 80, 85], combining a rectifier with a Dickson charge pump [55, 61, 85] to amplify the rectified voltage and store it on a capacitor. The capacitor's charging behavior reflects variations in the incident RF power, enabling estimation of path loss and soil moisture (Section 3.2). To ensure sensitivity at low incident powers while still reaching V_{Thresh}, we carefully optimize the capacitor value and the number of Dickson stages. Smaller capacitors charge more quickly, but this fast response can mask subtle differences between closely spaced incident power levels. Conversely, larger capacitors provide better resolution of incident power changes but may fail to reach V_{Thresh} under low RF conditions. Similarly, increasing the number of voltage-doubling stages boosts the output voltage and improves performance, but saturates beyond a certain point [2, 6, 60, 80].This trade-off is illustrated in our LTSpice simulations (Fig.2), where the output voltage improves up to 12 stages and then begins to degrade.[†] We select the capacitor and stage count to ensure that the EC voltage reliably crosses V_{Thresh}, even at low incident powers (higher moisture). More details on the choice of design parameters and components are provided in Section4.

Energy Sensing Block: The Tags monitor the EC voltage across the storage capacitor (33μF) to determine when it reaches a predefined threshold (V_{Thresh}). A simple approach is to use a comparator that continuously compares the capacitor voltage against a reference voltage (V_{Thresh}); however, such a comparator remains always on and would consume constant power (approximately 8 μW). To avoid this, we incorporate a load switch, which remains "off" until the capacitor voltage reaches the turn-on threshold of the switch (V_{ON}). When the capacitor voltage is below V_{ON}, the switch remains open, drawing negligible current. Once the capacitor voltage exceeds V_{ON}, the switch closes, connecting the battery to the microcontroller and thereby turning it on. Therefore, the turn-on voltage of the switch determines the minimum voltage that can trigger a response. Thus, despite using a microcontroller and an active radio, by incorporating an ultra-low-power switch [76], the overall power consumption of this block is low enough to be powered by a coin cell battery while supporting an operational

[†]Due to long simulation times, we simulate at 10MHz for 500ms.

lifetime of 16 years under ideal conditions.[‡] We evaluate the battery life of the Tag in more detail and provide realistic estimates in Section 5.7.

Active Response Block: The final and integral block of EC-Sense Tags is the active response block, which contains the microcontroller–radio pair. Unlike backscatter tags, EC-Sense Tags send an active response: the microcontroller configures the radio and triggers it to respond with TAG-MSG as soon as the energy sensing block is activated. Since the propagation time of radio signals is negligible, the active response time (ART)—defined as the time difference between the broadcast from the RF Source (SRC-MSG) and the arrival of TAG-MSG at the Source—is approximately equal to the EC time of the Tag. For accurate ART estimation, we design TAG-MSG to be a short (16-bit), FSK-modulated, narrowband (25 kHz) message that is predetermined and hard-coded. Despite transmitting TAG-MSG over a narrow band, we achieve high-resolution ART estimates, as they are independent of the bandwidth. We design the baud/bit rate of the response to optimize the trade-off between radio energy consumption and the accuracy of detection at the Source (evaluated in Section 5.8). We assign a unique TAG-MSG to each of the surface and buried Tags so that the Source can differentiate between the responses and estimate the ART for each Tag individually.

3.2 Path Loss Estimation Using Active Response Time

The second challenge in building EC-Sense is estimating the incident power at the Tags—and, in turn, the path loss experienced by the RF signals. Existing works utilize antenna arrays or ultra-wideband radios to determine RTT [10, 20, 43, 45] with nanosecond accuracy. Our approach is to estimate path loss from the EC time of the Tags. We evaluate the consistency of EC time with respect to incident power, across multiple Tags and with a single Tag operating in air vs. buried environment, using wired experiments. Figure 3 shows the EC time of our standalone energy capture circuit at varying incident powers. We can observe that the EC time is a direct indicator of incident power. Variations in the EC times are large enough to distinguish incident power differences as small as 1dBm, resulting in high-resolution soil moisture measurements. As discussed earlier, the Energy Capture (EC) time is approximately equal to the Active Response Time (ART), since the RF signal propagation delay is negligible at short distances (less than 1m). Therefore, we use the terms EC time and ART interchangeably throughout this section.

Determining Active Response Time in EC-Sense: We implement the ART measurement algorithm on the RF Source, which can transmit and receive concurrently at different frequencies. Upon initiating the SRC-MSG transmission, the Source turns its receiver ON and listens for TAG-MSG while continuing to transmit. SRC-MSG and TAG-MSG are sent on different frequency bands and thus do not cause self-interference at the Source. The Source receives two distinct responses—one from the surface Tag and one from the buried Tag. We distinguish between the two by assigning a unique 16-bit sequence to each Tag. Since the surface Tag is closer to the Source, the incident power at the surface Tag is always higher than that at the buried Tag. Therefore, the response from the surface Tag arrives first, followed by the response from the buried Tag. The Source measures ART by calculating the number of samples elapsed between sending the SRC-MSG and receiving the TAG-MSG. With prior knowledge of the system's sampling rate, the accurate time difference is computed. The Source keeps track of the TAG-MSGs from both Tags, and the respective ART values are given as input to the path loss estimation algorithm.

Path Loss Estimation: To the best of our knowledge, there is no closed-form function that defines the relationship between EC time and incident power; this requires further study and is beyond the scope of this work [4, 39, 72]. We therefore determine this relationship experimentally. Specifically, we measure the EC time by connecting the Source, followed by an attenuator, to the input of the EC circuit using wires. With precise control of the Source output power, we vary the incident power at the Tag from −17 dBm to +10 dBm. The measured EC times are

[‡]Assuming 10 activations per day.

shown in Figure 3. Since propagation delay through wires is negligible, the time calculated in this experiment reflects solely the EC time of the circuit. It is important to note that this calibration is general-purpose and only needs to be performed once for a given Tag design. The results in Figure 3 show that EC times are consistent across multiple Tags. To further evaluate the impact of the medium in which the Tag is placed, we conduct experiments to verify whether the relationship between EC time and incident power holds when the Tag is placed in soil. As shown in Figure 4, the results confirm that ART variations are solely due to changes in incident power, and that the surrounding medium (air or soil) has no impact on the measurement. We leverage this relationship in our wireless experiments to estimate path loss and, consequently, infer soil moisture. The path loss L experienced by the radio signals from the Source to each Tag is then determined using prior knowledge of the Source transmit power P_{Tx} and the estimated incident power P_{incident}, as: $L = P_{Tx} - P_{incident}$.

3.3 Measuring Soil Moisture from Pathloss Estimates from Surface and Buried Tags

We use the path loss estimates from both Tags—along with their relationship to distance and the propagation medium—to measure soil moisture. The surface Tag, as shown in Figure 5, receives the radio signal propagated only through the air medium from the Source. Therefore, the path loss estimate L_1 from the surface Tag can be modeled using the Friis equation [27]. The path loss L_2 between the Source and the buried Tag is more complex; it is a function of three components: (1) L_{s_ats} — spreading loss from air to soil, (2) L_t — transmission loss due to attenuation in soil, and (3) L_r — refraction loss. L_2 can thus be expressed as:

$$L_2 = L_{s_ats} \times L_t \times L_r \tag{1}$$

The spreading loss accounts for the distance in air (d_{a2}), the distance in soil (d_s), the attenuation coefficient α, and the shorter wavelength in soil caused by the phase coefficient β (more details in the Appendix). Combining α, β, and well-known models for path loss [82], we derive the spreading loss from air to soil as:

$$L_{s_ats} = \frac{1}{G_t G_r}\left(\frac{4\pi(d_{a2} + d_s\sqrt{\epsilon_a})}{\lambda_0}\right)^2 \tag{2}$$

Transmission loss is given by $L_t = e^{2\alpha d_s}$, and refraction loss is given by $L_r = 1/T$, where T is the transmittance—the fraction of incident power refracted into the soil from the surface. When the wave reaches the air-to-soil interface, it undergoes both reflection and refraction, making the overall path loss L_2 more complex. To simplify, we consider the special case of normal incidence, where the Source is placed right above the Tags. Then, $d_{a1} = d_{a2} = h_a$ and $d_s = h_s$ and the path loss from the Source to the surface and buried Tags L_1 and L_2 respectively are given by,

$$L_1 = \frac{1}{G_t G_r}\left(\frac{4\pi h_a}{\lambda_0}\right)^2 \tag{3}$$

$$L_2 = \frac{1}{G_t G_r}\left(\frac{4\pi(h_a + h_s\sqrt{\epsilon_a})}{\lambda_0}\right)^2 L_t L_r \tag{4}$$

where $L_t = e^{2\alpha h_s}$ and $L_r = 1/\left(1 - \left|\frac{1-\sqrt{\epsilon_a}}{1+\sqrt{\epsilon_a}}\right|^2\right)$.

We use our path loss estimate in air from the surface Tag L_1 to remove the impact of air-to-soil on L_2 and determine the path loss in soil alone. Furthermore, it has been documented that the experimental path loss estimates have an offset from theory due to environmental conditions [35, 54], and is variable [44, 58]. We use the difference between the experimentally determined path loss from the surface Tag $\hat{L}_1$ and its theoretical estimate L_1 as $\Delta L = \hat{L}_1 - L_1$ to compensate for this offset. Since both Tags are in the same environment, we use ΔL to calibrate $\hat{L}_2$, the experimental path loss from the buried Tag, i.e.,, $\hat{L}'_2 = \hat{L}_2 - \Delta L$.

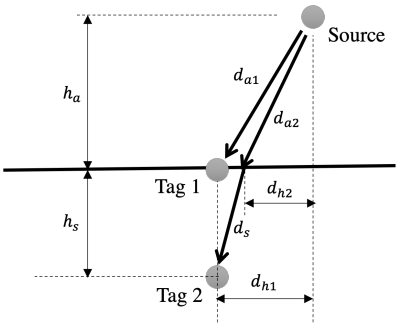

Fig. 5. Model of spherical wave propagation from the Source to two tags, one on the soil surface and the other buried.

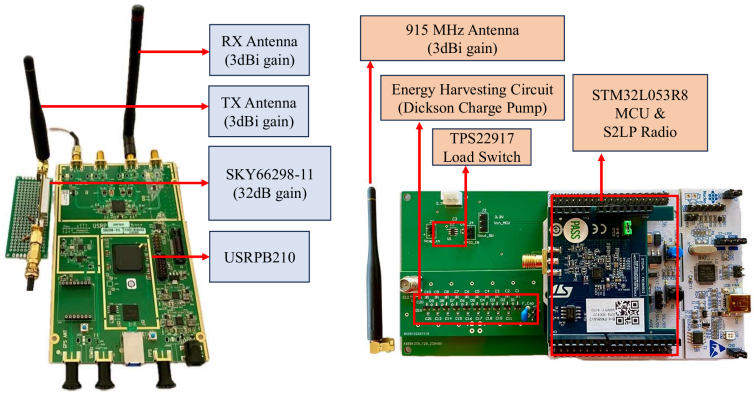

Fig. 6. EC-Sense Implementation: (a) Source consisting of a USRPB210, a power amplifier, and a 3 dBi whip antenna; (b) Ultra-low-power Tag that captures energy onto a 33 μF capacitor and uses a load switch for sensing to activate an STM32 microcontroller and radio, transmitting a 16-bit response.

$\hat{L}_2'$ (or $\hat{L}_2$) captures the effect of soil attenuation and hence soil moisture, as given by Equation 4. The theoretical path loss L_2 is a function of system parameters such as antenna gains G_t and G_r, wavelength in air λ, Source height h_a, and the depth of the buried Tag h_s, as well as soil properties such as the attenuation coefficient α and the real part of soil permittivity ϵ_r'. All except α and ϵ_r' are known *a priori*. Therefore, we formulate that, given the system and the measured path loss, soil moisture θ minimizes the difference between the measured, calibrated path loss $\hat{L}_2'$ and the estimated path loss L_2. Since $\hat{L}_2'$ is a non-linear function of θ, we redefine this as an optimization problem as follows,

$$\hat{\theta} = \underset{\theta \in [0,1]}{\arg\min} \left| \hat{L}_2' - L_2 \right| \tag{5}$$

where $[0, 1]$ is the normalized range of soil moisture, which is a function of the soil type [34, 36]. We notice that in the valid range of θ, both α and ϵ_a increase monotonically with θ, resulting in L_2 increasing monotonically with θ. Therefore, Equation 5 has only one solution for a given measured path loss, $\hat{L}_2'$.

In summary, EC-Sense measures the active response time (ART) using an energy capture circuit and estimates the incident powers and path loss experienced by both Tags. The path loss values are then used to minimize Equation 5, yielding the corresponding soil moisture value. By using a two-Tag setup, EC-Sense eliminates the effects of environmental variations and isolates the impact of soil.

4 IMPLEMENTATION

We implement and evaluate EC-Sense using SDRs as RF Source and a PCB implementation of ultra-low-power Tags in soil. We describe the hardware and software implementations of each module in detail below. PCB and software files to recreate EC-Sense are made publicly available on the anonymized GitHub page.[§]

4.1 Source Implementation

The RF Source (Figure 6(a)) is responsible for sending SRC-MSG to the Tags, receiving their responses, and measuring soil moisture from the estimated ART. We implement these functions using the USRP B210 [67], a

[§]https://anonymous.4open.science/r/ECSense-System/

full-duplex SDR frontend, connected to an Intel Core i7 4.2 GHz laptop with 16 GB RAM. The transmit module of the Source sends a continuous 1 kHz cosine signal (single tone) centered at 902 MHz for a specific duration. Using the SKY66298-11 EVB power amplifier (32 dB gain) [71] and a 3 dBi gain quarter-wave whip antenna, the total Effective Isotropic Radiated Power (EIRP) is 35 dBm. We choose a sampling rate of 9.6 Msps to achieve nanosecond-scale resolution (~104 ns between samples), enabling precise measurement of the Active Response Time (ART). In parallel, the receiver listens for TAG-MSG at 915 MHz. The received samples are stored and processed to estimate the ART. The Tx and Rx code is written in Python, utilizing multithreaded operations for full-duplex operation on the USRP. The Source can also be implemented on any general-purpose, multi-channel radio front-end such as LimeSDR [50] or BladeRF [62].

4.2 Tag Implementation

Figure. 6(b) shows our Tag with the following three blocks.

(a) Energy Capture Block : The EC block consists of a half-wave rectifier followed by a 12-stage Dickson charge pump. We utilize low forward voltage drop (350 mV) SMS7630 Schottky diodes [37] to minimize losses. To ensure maximum power transfer from the antenna to the EH block, we implement an LC matching network. Utilizing the Smith chart utility within ADS, we design the LC network to match the input impedance of the circuit to the antenna impedance. Using LTSpice simulations we determine that increasing the number of voltage doubling stages increases the voltage amplification, but saturates beyond 12 [2, 60, 80]. Therefore, we choose 12-stage doubling circuit to be a good trade-off. We employ a 33 μF capacitor for energy storage at the end of the 12th stage, chosen to meet the required voltage threshold at lower incident powers.

(b) Energy Sensing Block: We implement energy sensing using Texas Instruments' TPS22917 [76] ultra-low leakage load switch. The switch consumes approximately 0.08 μA in the OFF state and around 1 μA when ON. It supports input voltages ranging from 1 V to 5 V and features a turn-on threshold (V_{ON}) of 1 V. Although the datasheet specifies a turn-on voltage of 1 V, in our experiments the switch turned on at approximately 650 mV. When the voltage at the EN (enable) pin exceeds V_{ON}, the switch closes, passing the input voltage to the output. The switch turns off when the EN pin voltage drops below the turn-off threshold (V_{OFF}), which is approximately 250 mV. In our design, the EN pin is connected to the storage capacitor of EH. When the harvested voltage reaches V_{ON}, the switch turns on, and its output is fed into the V_{IN} of the microcontroller, enabling the MCU.

(c) Active Response Block: For the active response, we use the ultra-low-power STM32L053R8 microcontroller from STMicroelectronics [75] in conjunction with the S2LP transceiver [73]. The STM32L0 consumes approximately 88μA/MHz in active mode, while the S2LP radio draws around 5.8 mA when transmitting at 0 dBm output power. All experiments are conducted using the STEVAL-FKI868V2 evaluation kit [74]. To minimize current consumption, we remove the onboard debugger from the evaluation board. Once the microcontroller and transceiver are powered on, they are configured to immediately transmit a 16-bit response using frequency-shift keying (FSK) modulation, centered at 915 MHz with a data rate of 24 kbps. Communication between the microcontroller and the radio is handled via the SPI interface. To maintain ultra-low-power operation, the microcontroller enters low-power sleep mode immediately after the radio transmission is complete. The radio always transmits at 0 dBm output power in our implementation.

We experimentally measured the current profile of our Tag using a Keysight multimeter and BenchVue software. As shown in Figure 7, the Tag operates in three phases: (a) Energy Capture, where the capacitor charges and current is near zero; (b) Energy Sensing, where the TPS22917 load switch activates, consuming only 0.8 µA; and (b) Active Response, where the MCU and radio draw 5.8 mA for 1.7 s, consuming 32 mJ of energy per activation. Because soil moisture changes slowly, we assume the Tag activates only 10 times per day (moisture reading is taken 10 times in a day). Based on this duty cycle, the average daily energy consumption is 320 mJ, leading to an estimated average power draw of 3.7 µW. With a standard 220 mAh coin cell (CR2032), the Tag can operate

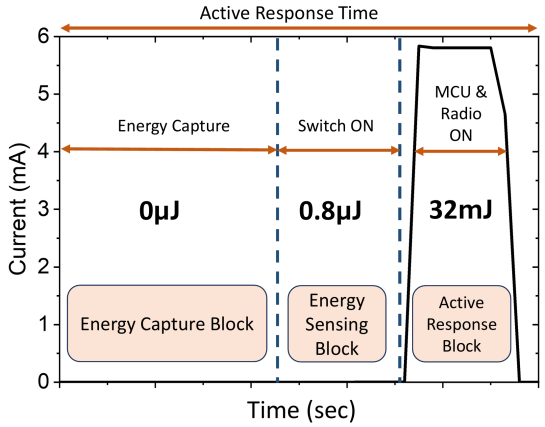

Table 2. Tag power consumption assuming 10 activations per day.

Block	Energy (mJ)	Power (μW)
Energy Sensing	0.0008	0.00001
Active Response	32	3.70
Total	**32.0008**	**3.70**

Fig. 7. Current consumption of the Tag during different operational phases. Energy values are annotated for each block.

for over 16 years. However, this estimate assumes ideal conditions and does not account for real-world factors like self-discharge or underground environmental stress. We conservatively estimate the practical lifetime to fall between 5–10 years under moderate temperature conditions, and approximately 2 years under cold extremes (e.g., near 0 °C). More detailed analysis of battery life across different measurement frequencies and deployment scenarios is presented in Section 5.7.

4.3 Cost Analysis

EC-Sense Tag: Our current prototype uses off-the-shelf components, including the STEVAL-FKI868V2 evaluation board [74] ($69) and a commercial whip antenna [51] ($6). Including the energy harvesting components (diodes, capacitors, resistors – approx. $3) and PCB fabrication (approx. $2), the total cost per prototype Tag is approximately $80. While suitable for development and testing, this cost is not viable for large-scale deployment. In a custom design implementation, we envision using a low-power microcontroller with an integrated sub-GHz radio (e.g., TI CC1310 [77] – $2), a PCB-etched antenna, and a compact energy harvesting circuit (approx. $3 for components). Including PCB fabrication (approx. $2), the total cost of a custom Tag is estimated to be approximately $8–$10 per unit.

Source : The core functionality of the Source is to transmit and receive simultaneously on two separate frequencies using a shared clock or within a single device. This functionality can be implemented using off-the-shelf SDRs such as the LimeSDR Mini [50](≈$150) or BladeRF[62] (≈$450), both of which support concurrent TX/RX. Alternatively, a custom design using two synchronized CC1125 transceivers [38] (each ≈$6) controlled by the same MCU is also feasible, offering a lower-cost path for large-scale deployments. Our current prototype uses USRP for the ease of programming and due to its availability in academic labs.

5 EVALUATION

We evaluate EC-Sense experimentally through various real-world experiments at a variety of locations and soil types with two Tags and USRP as Source. In this section, we answer the following questions towards evaluating the feasibility, correctness, and performance of EC-Sense.

- How well does EC-Sense perform in real world deployments, with varying environmental conditions?(Sec. 5.2)
- What is the impact of differential sensing on EC-Sense accuracy? (Sec. 5.2)
- How does EC-Sense perform with varying soil types at different Tag depths? (Sec. 5.3)
- Does the accuracy of moisture estimation vary with the time of measurement?(Sec. 5.4)
- Can EC-Sense Tags reach the depths necessary for soil moisture analysis? (Sec. 5.5)

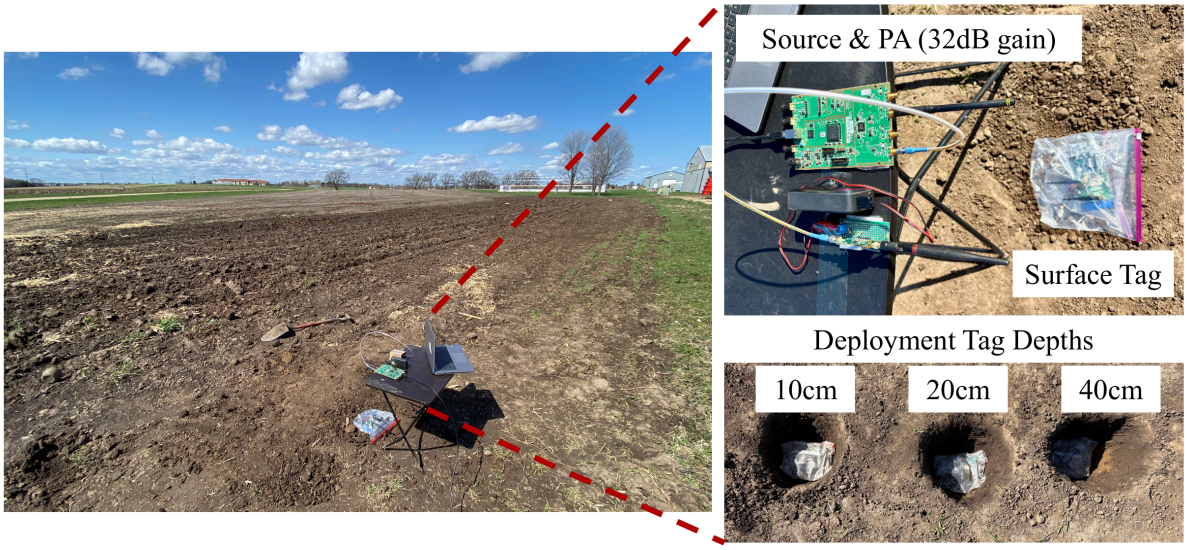

Fig. 8. EC-Sense outdoor field deployment setup with Source, surface, and buried Tags at 10 cm, 20 cm, and 40 cm depths.

- How well does ART capture the variations in path loss? (Sec. 5.6)
- What is achievable battery-life of EC-Sense Tags? (Sec. 5.7)
- What are the tradeoffs in active radio design? (Sec. 5.8)
- How is EC-Sense resilient to Source and Tag misalignment? (Sec. 5.9)

5.1 Experimental Setup

We evaluate EC-Sense in three different settings : (i) an agricultural field, and (ii) an outdoor lawn with silt loam soil, and (iii) an indoor setup with sandy loam and silty clay loam soil. In the agricultural field (Figure 8), we deploy Tags at depths of 10 cm, 20 cm, and 40 cm, and measure moisture over the course of one week. In the outdoor lawn experiments, we vary the soil moisture levels and evaluate EC-Sense's resilience to environmental changes. In the indoor lab setting, we perform controlled moisture experiments. We saturate the soil with water and measure moisture levels periodically until the soil is dry. We observe the results at a Source height of 30 cm and 50 cm above the ground and Tag depths of 10 cm, 15 cm, 20 cm, and 30 cm below the ground.
To adapt EC-Sense to a particular soil type, we update the sand, silt, and clay percentages, along with the soil's bulk density, in the moisture estimation algorithm. These parameters influence the soil's dielectric properties and its impact on signal attenuation, which are central to the pathloss-to-moisture mapping in our model. The required values for soil composition and density are well-documented in soil science literature and readily available through USDA databases [84] and prior studies, making EC-Sense easily configurable for a wide range of deployment environments.
Baselines Compared: We measure the ground truth using METER's TEROS 12 Advanced Soil Moisture Sensor [33] that uses EM signal to measure the dielectric permittivity of the surrounding medium.

5.2 EC-Sense in Open Field Deployments

To evaluate the performance of EC-Sense in practical settings, we deployed Tags at depths of 10 cm, 20 cm, and 40 cm over the course of one week in silt loam soil in an outdoor field. The RF Source was placed at a fixed height of 50 cm above the ground, and measurements were taken twice per day. For each measurement, we first recorded

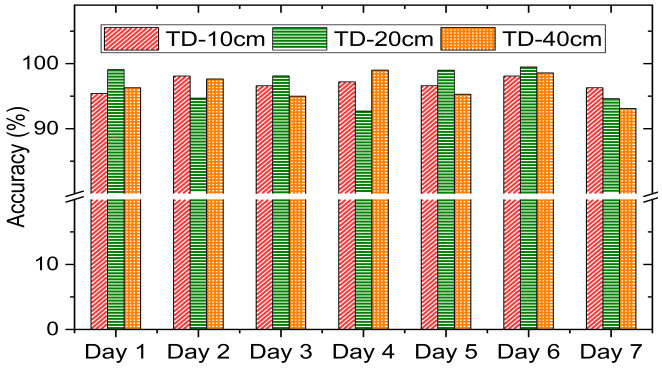

Fig. 9. EC-Sense moisture measurements with Tags deployed at 10 cm, 20 cm and 40 cm depths over a week.

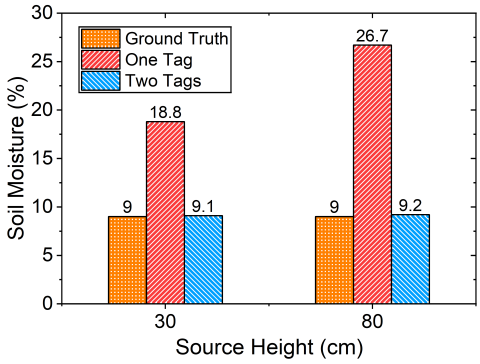

Fig. 10. Impact of differential sensing using surface Tag on the accuracy.

the ground truth soil moisture at each Tag depth, followed by a measurement using the EC-Sense system. Figure 9 shows the accuracy in moisture measurement using EC-Sense Tags across different days. EC-Sense reports an average accuracy of 98% across all the experiments, demonstrating reliable performance in practical settings. A key takeaway is our system's robustness and resilience—during the one-week period, we observed significant variations in outdoor conditions, including heavy wind, rain, and changes in temperature and humidity—and EC-Sense maintained reliable accuracy throughout.

Impact of Differential Sensing on Path Loss Compensation: We attribute the resilience of EC-Sense to the differential sensing using the surface Tag, which compensates for the path loss in air. The difference between the path loss estimate from the surface Tag and the theoretical estimate using Friis' equation (Section 3.3) helps account for the environmental impact on the buried Tag. Figure 10 shows a snapshot of our experiments at a moisture level of 9% with two different Source heights. The estimated soil moisture using a single Tag (red bars) is highly dependent on the Source height, as variations in the air medium have a direct impact on the path loss estimate. In contrast, the accuracy of soil moisture estimation using two Tags (blue bars), where the surface Tag estimates are used to compensate for environmental variation, is unaffected by changes in Source height and remains closest to the ground truth. Thus, the use of the surface Tag for compensating the air medium is critical in measuring soil moisture from buried Tags, as it isolates the soil properties from the overall path loss.

5.3 Generalizability of EC-Sense in Different Soil Types

To evaluate the generalizability of EC-Sense across a broad spectrum of soil conditions, we perform controlled indoor experiments with three representative soil types—Silt Loam, Sandy Loam, and Silty Clay Loam—each with distinct textural compositions. Silt Loam contains ~70% silt and 10–20% clay, Sandy Loam is dominated by ~60–70% sand, and Silty Clay Loam has the highest clay content at ~30–35%. These variations influence both soil permittivity and RF attenuation, making them ideal for testing the adaptability of our system. For each soil type, we deploy EC-Sense Tags at depths of 10 cm, 20 cm, and 30 cm, and vary moisture levels from dry to saturation, while maintaining a fixed RF Source height of 50 cm.

Figure 11 presents the estimated moisture versus ground truth for each depth and soil type: (a) Silt Loam, (b) Sandy Loam, and (c) Silty Clay Loam. The shaded regions demarcate agriculturally important moisture bands—Dry, Total Available Water (TAW), Field Capacity (FC), and Saturation (Sat)—highlighting the system's ability to operate across the full moisture range. The region of most interest is typically TAW; when the soil moisture rises above field capacity or falls too low (dry region in the figure), finer resolution in moisture estimation is not needed. Notably, across all three soil types, EC-Sense consistently achieves high accuracy across depths and moisture

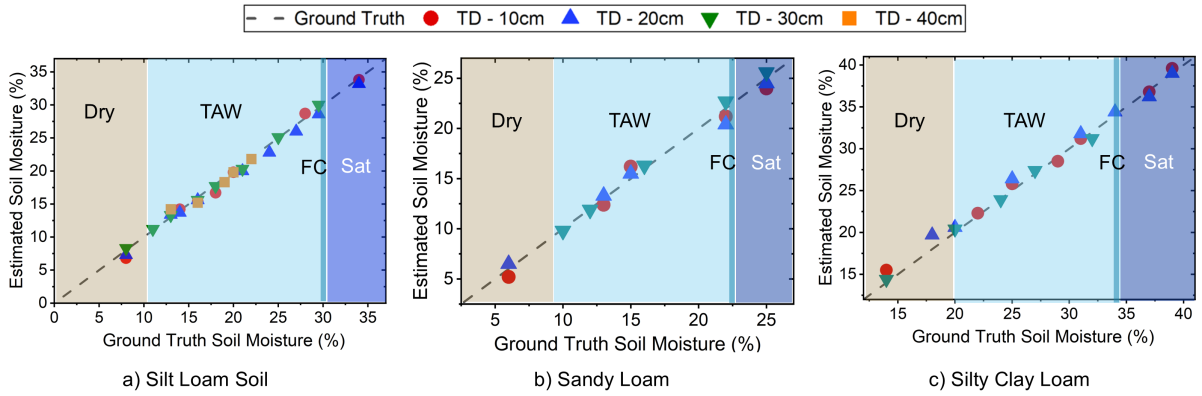

Fig. 11. Accuracy of EC-Sense across different soil types: (a) Silt Loam, (b) Sandy Loam, and (c) Silty Clay Loam. Shaded regions represent soil moisture zones—Dry, Total Available Water (TAW), Field Capacity (FC), and Saturation. TAW is the plant-available range between permanent wilting point (PWP) and FC.

levels, with an average accuracy of 99%. This demonstrates that EC-Sense maintains strong performance and generalizability across soils with varying dielectric and attenuation characteristics—a key challenge in real-world deployments.

5.4 EC-Sense in a Controlled Indoor Environment

To further evaluate the resilience of EC-Sense, we perform controlled experiments indoors to benchmark the individual components. Here, we evaluate the consistency of our soil moisture measurements over time. We measure in-situ soil moisture every two hours over a 24-hour period without any human intervention in our indoor lab setup. We saturate the soil with water, mix it thoroughly, and program the USRP to transmit a SRC-MSG every two hours, followed by soil moisture measurements that are stored on the laptop connected to it. This experiment ensures uniform water distribution and emulates a real-world scenario of soil drying after rainfall. We fix the Source height to 30 cm and the Tag depth to 15 cm.

Figure 12 shows the soil moisture measured by EC-Sense (red bars) and compares it with the ground truth (blue). For sandy loam soils, the moisture levels peak at approximately 25% [28, 43] and do not cover the full range of [0, 1]. Therefore, the moisture values decrease from 25% to 7% over time as the soil transitions from wet to dry over time. EC-Sense closely tracks the ground truth moisture values throughout the experiment, demonstrating high correlation and consistency over time. It is interesting to observe that the rate of decrease is higher in the beginning and is more gradual over time. This is due to rapid drying initially, which then slows down as moisture levels decrease [8].

5.5 Maximum Tag Depths Achieved: An Experimental and Analytical Analysis

Understanding the maximum sensing depth is critical for evaluating the usability of EC-Sense; this depth varies with soil type and moisture conditions. We perform controlled experiments on different soil types and moisture levels to determine the maximum depth at which EC-Sense Tags can successfully estimate soil moisture. We consider two key agronomic thresholds—Field Capacity (FC) and Saturation (Sat)—across three representative soil types: Sandy Loam, Silt Loam, and Silty Clay Loam. The FC and Sat levels are 22% and 25% for sandy loam, 30% and 35% for silt loam, and 34.5% and 40% for silty clay loam, respectively [14, 28].

Figure 13 shows the maximum depth achieved with the RF Source placed 50 cm above the soil surface. At this Source height, EC-Sense detects soil moisture accurately up to 40 cm depth at both FC and Sat (with theoretical

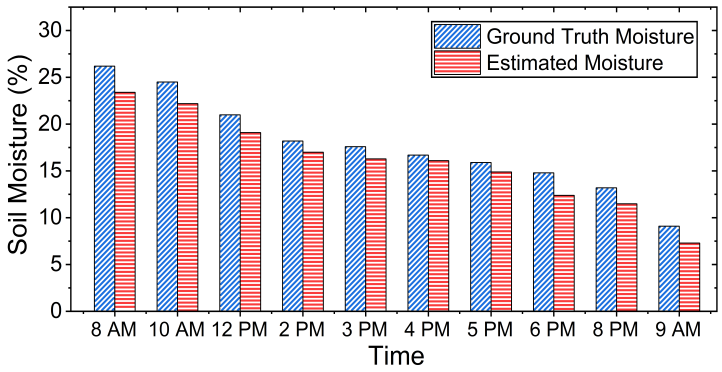

Fig. 12. EC-Sense moisture measurements over 24 Hours with a Source height of 30 cm and Tag depth of 15 cm.

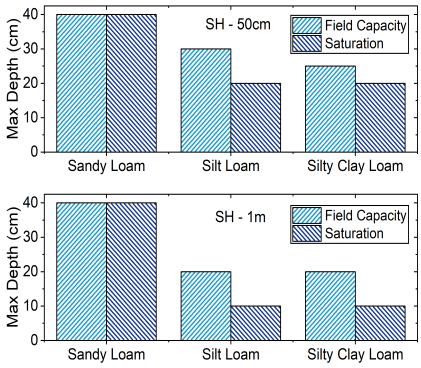

Fig. 13. Impact of Source height on max depth at FC and saturation.

estimates of 60 cm for FC and 50 cm for Sat) for sandy loam soil. For heavier soils like silt loam and silty clay loam, which exhibit higher dielectric losses, the maximum depth is lower—reaching up to 30 cm and 25 cm at FC, and 20 cm at Sat. To further evaluate the feasibility of drone- or rover-based deployments, we repeat the experiments with an increased Source height of 1 m (Figure 13). The increased distance results in additional path loss and reduced incident power at the buried Tags, lowering the maximum achievable depth. In this setting, sandy loam still allows sensing up to 40 cm (with theoretical estimates up to 50 cm at FC and 40 cm at Sat), whereas silt loam and silty clay loam are limited to 20 cm at FC and 10 cm under Sat.

We would like to note that accurate sensing up to field capacity (FC) is sufficient for precision agriculture, as it marks the soil's maximum water retention useful to plants. Irrigating beyond FC is avoided to prevent nutrient leaching and environmental runoff [14, 28]. EC-Sense 's ability to sense moisture up to—and slightly beyond—FC, even in high-clay soils, demonstrates its practical suitability. Sensing at 30–40 cm depths also aligns with the effective root zones of many major crops [22, 83], making EC-Sense ideal for long-term, low-power soil moisture measurements.

Achievable Tag Depths (Theoretical Estimation): The maximum operational depth of EC-Sense Tags depends on their ability to harvest sufficient RF energy at that depth. This depth can be improved by lowering the energy sensing threshold (V_{Thresh}), extending the SRC-MSG duration, or using higher-gain antennas. Figure 14 presents analytical estimates of the achievable depths under field capacity (FC) conditions—defined as the maximum moisture content useful to plants [14, 28]. We consider three representative soil types with different FC levels: 22% for sandy loam, 30% for silt loam, and 34% for silty clay loam. At each depth, we compute the soil-dependent path loss and the corresponding incident RF power at the buried Tag. The dashed line in Figure 14 represents the minimum power required to trigger the response (−22 dBm), based on a 200 mV threshold using a low-voltage ALD110802 load switch [17]. Based on this model, EC-Sense can theoretically support maximum depths of **50 cm in sandy loam**, **35 cm in silt loam**, and **30 cm in silty clay**.

These depth limits are primarily constrained by the incident RF power required to generate V_{Thresh}. Our current design uses a Dickson charge pump with SMS7630 diodes and achieves operation at −22 dBm (with 200 mV switch). However, future improvements—such as tighter antenna–rectifier matching [64] or the use of CMOS-based active rectifiers [49, 85]—could push the threshold even lower (e.g., −24 dBm), thereby extending EC-Sense 's depth.

5.6 Active Response Time and Its Impact on Path Loss Estimation

The accuracy of soil moisture measured by EC-Sense depends on the accuracy of ART measurements, which in turn determine the accuracy of path loss estimation. In Figure 15, we plot the ART of the surface and buried Tags

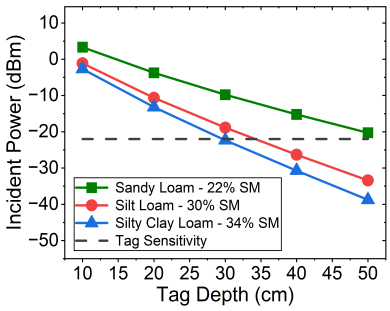

Fig. 14. Achievable Tag depths of EC-Sense for varying soil types.

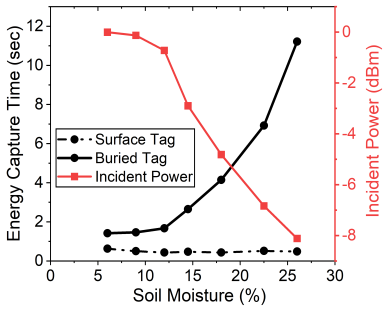

Fig. 15. Energy Capture Time and incident power of Tags vs moisture.

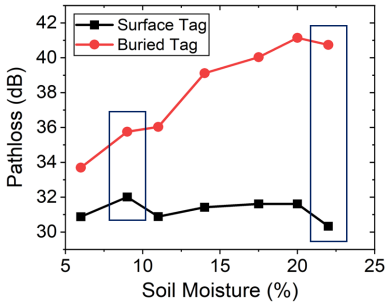

Fig. 16. Estimated path loss from EC-Sense Tags vs moisture.

at various soil moisture levels. We also plot the corresponding estimated incident power at the buried Tag (red line with square markers). Since the incident power at the surface Tag does not change with moisture, we do not plot it here. We note that the measured time to charge for the surface Tag (dotted line) remains relatively constant, as it does not depend on the soil and hence its moisture. The buried Tag, on the other hand, takes longer to charge (thick line with circle markers) as soil moisture increases. This is due to the increased attenuation losses in soil with increasing moisture; the estimated incident power at the buried Tag decreases accordingly. These results show that, in practical experiments, the charging time of the buried Tag is a strong function of soil moisture level.

In Figure 16, we plot the estimated path loss from the Source to the surface and buried Tags as a function of increasing soil moisture, at a Tag depth of 15 cm and a Source height of 50 cm. The path loss experienced by the surface Tag remains relatively flat across different moisture levels, while the path loss to the buried Tag increases with moisture. We highlight (in blue boxes) that whenever there is a sharp increase or decrease in the surface Tag's path loss, there is a corresponding change in the buried Tag's path loss as well. Since the radio wave to the buried Tag traverses both the air and soil media, it is affected by changes in the surface environment too. Thus, active response time (ART) as a measure of path loss is a unique and valuable metric for soil moisture estimation.

5.7 Battery Life of EC-Sense Tags

We design ultra-low-power Tags that are powered by batteries and buried underground. We experimentally measured the power consumption of EC-Sense Tags and estimated their expected battery life under varying measurement intervals. Figure 17 shows both the average power consumption (in μW) and the projected battery life (in years) as a function of the measurement interval. As expected, reducing the frequency of measurements significantly extends lifetime by lowering average power draw. For instance, taking measurements once every hour yields a projected battery life of approximately 10 years, while a 4-hour interval can extend this to nearly 30 years under ideal conditions with a coin cell battery (220mAh). However, real-world factors such as self-discharge, corrosion, and temperature-related degradation—especially in cold climates—can significantly impact performance. Based on these practical considerations, we conservatively estimate lifetimes in the range of 5–10 years under moderate conditions, and approximately 2 years in extreme environments (e.g., underground temperatures near 0 °C). Since soil moisture typically changes slowly, even a 4-hour measurement interval is adequate for most agricultural scenarios.

Comparison with Passive Backscatter Systems: Passive backscatter tags, such as those used in RFID systems, are often considered ultra-low-power since they operate without batteries. However, they still require incident RF energy to backscatter the signal, which imposes fundamental limitations. Backscatter tags face inherent challenges due to dual path loss (source-to-tag and tag-to-receiver), which becomes severe in lossy media like soil. For

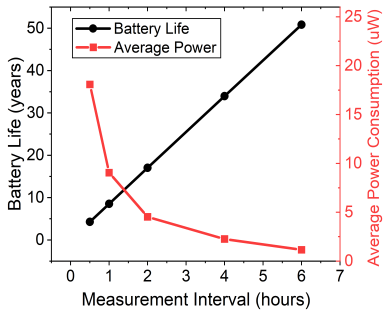

Fig. 17. Estimated battery-life of EC-Sense Tags with coin-cell battery.

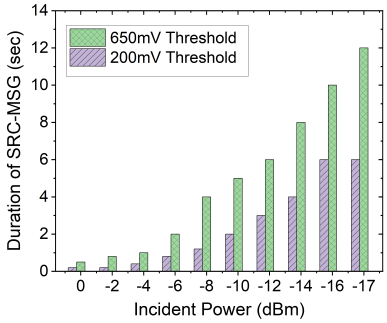

Fig. 18. Duration of SRC-MSG vs incident power.

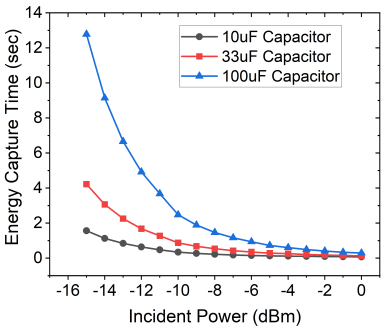

Fig. 19. EC time for different capacitor sizes.

instance, at 20% soil moisture (silt loam soil) and 20 cm depth with a 50 cm Source height, the round-trip path loss exceeds 90 dB—rendering signal recovery infeasible, especially under noise and environmental variability. This limits the maximum operational depth of backscatter tags to 5–10 cm [43, 86]. In contrast, EC-Sense uses an active radio, avoiding round-trip attenuation and enabling reliable operation at depths up to 30–40 cm. Additionally, EC-Sense consumes just 3.7 μW of average power and 32 mJ per measurement, compared to ~1–2 μJ per operation for passive tags [69]. This small energy cost provides substantial benefits in robustness, depth, and deployment flexibility—crucial for long-term in-situ soil monitoring.

5.8 Performance of Energy Capture from Radio Signals in Soil

The energy capture (EC) circuit plays a crucial role in the operation of EC-Sense. Here, we evaluate various parameters of the EC block and discuss our design choices. The EC block harvests energy from the radio signal transmitted by the Source (SRC-MSG). Since energy is defined as the product of power and time, the lower the incident power, the longer the duration needed to activate the Tag. In Figure 18, we plot the estimated duration for which the Source must transmit its SRC-MSG for the Tags to activate the radio and respond with TAG-MSG. In our experiments, to accommodate incident powers as low as −17 dBm, we send SRC-MSG for about 12 seconds. However, the required duration of the SRC-MSG also depends on the desired voltage of the EC circuit. Our Tag requires 650 mV at the capacitor for the switch to turn ON. With a lower-threshold switch [17], this requirement can be further reduced. For instance, lowering the threshold from 650 mV to 200 mV would decrease the SRC-MSG duration from 12 seconds to 6 seconds. Therefore, depending on the lowest expected incident power and the desired voltage, we design the duration of the SRC-MSG accordingly.

One of the critical design choices we make in the EC block is the selection of the storage capacitor. Since the charging time of the capacitor (or EC time) indicates the incident power, reliable estimates of charging time are essential. Figure 19 plots the charging time for three capacitor sizes: 10 μF, 33 μF, and 100 μF. We conduct wired experiments to measure the charging time under varying incident power. Although each capacitor exhibits an exponential relationship with incident power, the difference in charging time between two adjacent power levels plays a critical role in the resolution of soil moisture measurements. If the charging times are too close to one another, the number of distinct incident power levels—and hence, distinguishable soil moisture levels—will be reduced. However, larger capacitors demand longer charging times and thus longer transmission durations from the Source. Therefore, a trade-off between SRC-MSG duration and the desired soil moisture resolution must be carefully considered during practical deployments.

In our Tag design, we choose a 24 kbps bit rate for TAG-MSG to balance energy efficiency and bit error rate (BER). Lower bit rates reduce BER but increase energy consumption. Since our messages are short (16 bits) and

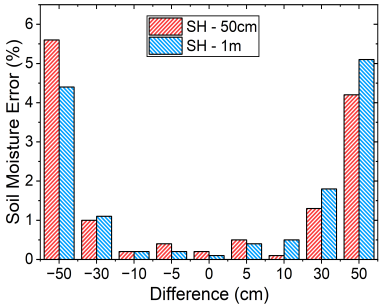

Fig. 20. Impact of lateral misalignment of Source w.r.t to buried Tag.

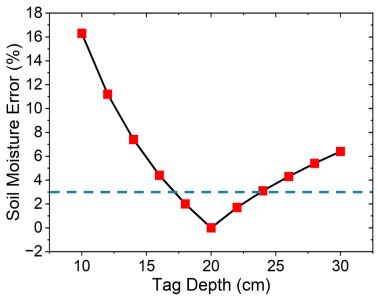

Fig. 21. Impact of Tag depth misplacement on moisture estimation accuracy.

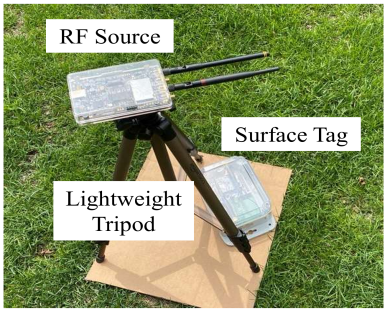

Fig. 22. Prototype deployment setup for EC-Sense with RF Source and surface Tag.

transmitted over short distances (<100 cm), the BER remains low even at 24 kbps. This choice minimizes energy consumption to a few μJ, which is crucial for ultra-low-power operation.

5.9 Impact of Source–Tag Misalignment on EC-Sense

Source Misalignment: In real-world deployments, we envision a drone or rover carrying the RF Source and surface Tag to measurement locations. With buried Tag positions pre-mapped, GPS can be used to align the Source above each Tag. However, GPS inaccuracies or mechanical offset may lead to lateral misalignment. To evaluate the impact, we experimentally shifted the Source laterally by up to 50 cm and measured the resulting soil moisture estimation error at Source heights of 50 cm and 1 m. As shown in Figure 20, estimation error remains under 2% for offsets up to 30 cm and increases to about 5% at 50 cm, with consistent trends across both heights. This is because small lateral shifts result in negligible changes in path loss near the center of the antenna's radiation pattern. Importantly, modern GPS technologies like Real-Time Kinematic (RTK) achieve 1–2 cm accuracy under good conditions [1, 31]. Integrating RTK with drones or rovers ensures near-perfect alignment. Since even 30 cm of misalignment introduces less than 2% error, EC-Sense remains robust and accurate under practical deployment conditions.

Impact of Tag Depth Misplacement: In real-world deployments, slight variations in the buried Tag's depth can occur due to manual installation errors, soil settling, or erosion. To evaluate the robustness of EC-Sense under such conditions, we perform simulations where the Tag depth is varied from 10 cm to 30 cm in 2 cm increments, and we measure the resulting soil moisture estimation error. As shown in Figure 21, the system achieves the highest accuracy at the calibrated depth of 20 cm, where the error is minimal (0%). Deviating from this depth leads to increasing errors, reaching over 16% when the Tag is at 10 cm and over 6% at 30 cm. This asymmetric error pattern highlights the sensitivity of the system to calibration depth. Notably, shallower depths exhibit larger errors because even small changes lead to significant variations in path loss due to stronger signal attenuation near the surface. In contrast, deeper deployments experience more gradual path loss variation, making them more robust to minor depth offsets. Still, EC-Sense maintains less than 5% error within ±5 cm of the intended depth, demonstrating good tolerance to deployment inaccuracies.

6 DEPLOYMENT DISCUSSION

6.1 Use of Autonomous Platforms for EC-Sense Deployment

EC-Sense is designed to work with mobile platforms such as drones and autonomous ground rovers commonly used in agricultural fields. We envision a lightweight assembly that integrates both the RF Source and Surface Tag

with a fixed vertical alignment between them—such as a simple tripod-like structure with the Source mounted at the top and the Surface Tag at the bottom. As illustrated in Figure 22, we envision a compact, reusable assembly that ensures fixed vertical separation between the RF Source and Surface Tag. This structure can be easily positioned by drones or rovers over buried Tags for scalable, autonomous soil moisture sensing. The assembly ensures that the distance between the Source and the Surface Tag remains constant; it can be autonomously lowered or placed near the surface for measurement and retrieved afterward, while the buried Tags remain in place. Therefore, to monitor a field, only a single Source and Surface Tag are needed, along with multiple buried Tags. Drones flying at 1–5 meters or rovers navigating the field can move to pre-mapped buried Tag locations using GPS and position the assembly in designated sensing zones—such as inter-row crop gaps—without disturbing the plantation. Each measurement uses the corresponding buried Tag at a fixed depth; the Surface Tag enables differential sensing by isolating the soil's contribution to path loss from that of the air, making the system robust to environmental variations. Importantly, a single Surface Tag can be reused across many buried Tags, reducing deployment complexity.

Use of a drone or rover has the potential to cause lateral misalignment. We experimentally evaluated the impact of such misalignment. We show that EC-Sense maintains high accuracy even with Source offsets up to 30–50 cm (Section 5.9). Furthermore, GPS navigation with Real-Time Kinematic (RTK) enhancements can achieve centimeter-level accuracy [1, 31], ensuring precise alignment. Robotic platforms such as AiGen [3], EarthSense [24], and FarmDroid [7] are already being used for in-field agricultural tasks and are well-suited to carry and deploy EC-Sense efficiently. Mobile deployment, along with its low-power design, enables EC-Sense to achieve long-term, wide-area soil moisture monitoring.

6.2 Managing Shift in Buried Tag Depths

Agricultural activities such as tilling, soil erosion, or seasonal land movement can cause shifts in the depth of buried Tags over time. Since the accuracy of EC-Sense depends on knowing the Tag's depth for path loss interpretation, such depth variations may introduce moisture estimation errors. We evaluate the impact of depth shifts via simulation and present the results in Section 5.9, showing that EC-Sense can tolerate moderate depth deviations (e.g., within ±4 cm) with less than 2% error.To improve robustness against these variations, we envision a simple yet effective deployment mechanism inspired by water level markers used at dams [16]. Specifically, the buried Tag can be mounted on a rigid vertical rod or scale that is inserted into the soil, with calibrated depth markings visible above the surface. This enables easy visual verification of the Tag's depth over time and allows field workers to periodically check or re-adjust the Tag's position if necessary. This low-cost solution can help ensure long-term accuracy and reliability of moisture measurements in dynamic agricultural environments.

In addition to mechanical stability, long-term durability also requires protecting the Tag from moisture and other corrosive compounds. While our current prototypes use double-layered airtight plastic bags for ease of deployment, for long-term field installations, we envision embedding the Tags in sealed, waterproof enclosures (e.g., epoxy-sealed capsules or IP-rated boxes) [66]. These housings would prevent water ingress, corrosion, and physical degradation, ensuring reliable operation over multi-year deployments.

7 LIMITATIONS AND FUTURE WORK

To the best of our knowledge, EC-Sense is the first attempt to use EC time to measure soil moisture. We identify a few limitations and possible future research enabled by this work below.

Tag Depths: Our current deployment uses Tags placed 40 cm below ground. It has the potential to be buried upto 50 cm depths with the use of lower threshold switches as discussed in Section 5.5. As the Tag depth increases, the duration of SRC-MSG that powers the Tags will increase (ref. Fig. 18). Tag depths can be further improved

by optimizing the impedance matching circuit to minimize losses in power transfer and transitioning from diode-based designs to CMOS [80, 85].

Type of Crops Supported: A plant's root characteristics decide the amount of soil moisture accessed by it. It is recommended to place sensors at depths 1/2 to 3/4 of root zones [22, 63]. EC-Sense Tags at 40 cm is thus beneficial for crops with root zones of up to 4 feet [22, 83]; a vast variety of grains and vegetables have root zones < 4 ft [22, 83]. Large fruiting trees and crops with deeper roots require a sophisticated sensing system.

Field-Scale Moisture Estimation: Combining moisture measurements from multiple Tags could help construct a heatmap and obtain insights into the heterogeneity of the field. Since EC-Sense Tags use an active radio to respond, multiple Tags can respond simultaneously using FDMA. Further analysis is needed on the number of Tags that can harvest energy from a single Source in one shot.

Tag Location: EC-Sense EC-Sense Tags are buried; the RF Source require the locations of the Tag to land above them.. We envision using GPS to mark the locations of buried EC-Sense Tags, along with physical stakes—a common practice in agricultural systems. A drone or rover can then use GPS to autonomously position itself above each buried Tag for moisture sensing.

Type of Soil and Long-Term Deployments: Currently, we performed experiments using sandy loam, silt loam and silty clay loam. Longer-term outdoor evaluation with more soil types will offer insights into other practical challenges.

Sensitivity to Low Transmit Power: EC-Sense relies on sufficient incident RF energy to activate the Tag. If the transmit power is too low relative to the pathloss (e.g., in highly lossy soils or at Source greater distances), the Tag may not harvest enough energy to respond, resulting in a loss of measurement capability. In our current design, the minimum required incident power at the Tag for activation is approximately −17 dBm.

Algorithm: Develop closed-form models for mapping EC time to incident RF power, and extend the algorithm to account for additional soil parameters—such as salinity, nutrient concentration, and compaction—that influence RF attenuation, thereby enabling multi-parameter environmental sensing alongside moisture.

Theoretical Insight: To better understand the dependence of EC Time on incident RF power, we can model the harvester using a simple energy balance. The storage capacitor must accumulate $E = 0.5\, C_{\text{store}} V_{\text{Thresh}}^2$ [70], charged at an average rate $P_{\text{charge}} = \eta P_{\text{in}}$. This yields the relation for EC Time (T_{EC}) as

$$T_{\text{EC}} \approx \frac{0.5\, C_{\text{store}} V_{\text{Thresh}}^2}{\eta P_{\text{in}}},$$

which highlights the inverse dependence of EC Time on incident RF power. Here, P_{in} denotes the incident RF power at the Tag antenna, V_{Thresh} is the threshold voltage, C_{store} is the storage capacitance, and η is the effective RF-to-DC conversion efficiency. Prior work has experimentally validated closed-form expressions relating charging time and incident power in wireless RF transfer systems [59]. However, deriving such a theoretical expression for a Dickson charge pump circuit remains an open challenge, which we will explore as a part of future work.

Source Power Consumption: The RF Source in EC-Sense transmits at 33 dBm output power using a power amplifier, drawing approximately 5 W. Since the Source is active only for a few seconds (6 seconds max in our implementation) during each measurement and remains off otherwise, the overall duty cycle is low. Moreover, the mobile platform such as a drone or rover carrying the Source can recharge during inactive times between measurements.

8 RELATED WORK

Commercial Soil Moisture Sensors: Commercial soil moisture sensors use various techniques such as resistance [13, 25], capacitance [32, 33], tensiometers [68], and heat-diffusion [89] to estimate moisture through indirect properties. For example, the resistance-based sensors use two probes to sense the resistance in soil, and the capacitive sensors leverages the relationship between capacitor charge time and soil dielectric permittivity. While some are low-cost, they often suffer from accuracy issues, degradation over time, or require frequent calibration. Others that are durable can be expensive ($100s of dollars per sensor) and power-hungry, making them unsuitable for large-scale or long-term deployments. Moreover, most systems rely on wired setups, limiting their scalability and flexibility for wireless, in-situ monitoring.

RF-based Soil Sensing: Traditional RF-based approaches for soil moisture sensing include satellite-based remote sensing and time-of-flight (ToF) methods. Satellite-based systems such as NASA's SMAP [26] and ESA's Sentinel-1 [9] enable large-scale, low-cost monitoring but are limited by low spatial resolution and shallow sensing depths (typically only a few centimeters), making them unsuitable for real-time, field-level applications. In contrast, ToF-based techniques such as Ground Penetrating Radar (GPR)[48] and Time Domain Reflectometry (TDR)[78] offer high spatial resolution and deeper sensing capabilities. However, they require large bandwidths (hundreds to thousands of MHz) and are expensive, often costing several thousand dollars, which limits their practicality for scalable agricultural deployments.

Recent efforts have explored a variety of RF-based technologies—such as RFID, Wi-Fi, LTE, LoRa, chipless tags, and radar backscatter—for soil moisture sensing [12, 20, 29, 41, 43, 45, 86, 87]. GreenTag [86] uses commodity RFID tags to measure the minimum response threshold, but the tags are placed outside the soil on plant pots, limiting applicability in real-world field deployments. SoilTAG [41] proposes a buried, chipless passive tag for fine-grained sensing, but its operation is confined to controlled indoor environments, limiting its generalizability. Wi-Fi and LTE-based systems such as STROBE [20] and LTE-Soil-Meter [29] rely on phase-based signal features to estimate moisture. While these systems demonstrate promising accuracy, they require buried active radios and wired infrastructure, increasing power consumption and deployment complexity. Furthermore, phase-based sensing methods are known to be highly sensitive to environmental variations, antenna orientation, and multipath effects. They often require complex protocols for phase unwrapping or referencing, and perform best under carefully controlled conditions [10, 20, 87], which limits their robustness in large-scale agricultural environments. CoMEt [45] estimates moisture through round-trip delay using high-bandwidth backscatter (150–300 MHz), achieving depths up to 38 cm. However, it requires custom radar infrastructure, precise calibration. SoilCares [87] combines LoRa signal features with VNIR spectroscopy for multi-parameter sensing, but uses several active components that limit its battery life and require multiple sensing modalities. MetaSoil [12] achieves the greatest reported sensing depth (up to 1 m) using mmWave radar and passive metamaterial tags. However, the signal reaches the sensor via buried air-filled tunnels with directive guides, thereby avoiding soil propagation entirely. This enables deep sensing but at the cost of invasive infrastructure and limited scalability. Additionally, MetaSoil relies on moisture-sensitive hydrogel patches that must be replaced periodically, raising concerns about long-term maintenance and durability. SoilId [21] uses UAV-mounted IR-UWB radar and buried passive reflectors, but requires high bandwidth (2GHz) and extensive offline deep learning, limiting real-time use and increasing system complexity.

In contrast, EC-Sense uses low-bandwidth (24 kHz), ultra-low-power buried Tags that decouple sensing from communication. Our system leverages energy capture time (EC time) to measure pathloss, enabling accurate moisture estimation. EC-Sense operates reliably across diverse soil types and moisture levels, supports sensing depths up to 40 cm, and is designed for scalable, long-term deployment with minimal calibration or infrastructure overhead.

9 CONCLUSIONS

We presented EC-Sense, a novel and practical framework for soil moisture sensing using wire-free, ultra-low-power buried Tags that estimate moisture from energy capture time. Our design decouples sensing and communication, enabling robust path loss estimation through differential measurements between surface and buried Tags. This architecture offers resilience to environmental variations and supports reliable operation at depths up to 40 cm for sandy loam soil. To our knowledge, EC-Sense is the first system to establish a quantitative relationship between energy capture time and soil dielectric properties. Extensive indoor and field experiments across multiple soil types demonstrate that EC-Sense achieves high accuracy (over 98%) and long-term feasibility with low power consumption. Our results highlight the promise of energy-capture-based sensing as a scalable, low-cost alternative for in-situ soil monitoring.

Acknowledgments

We would like to thank our area editor and the anonymous reviewers for their valuable comments that helped us improve the paper. We are grateful to Prof. Jingyi Huang and Prof. Mallika Nocco for generously providing lab space and equipment to conduct soil experiments. We also thank Prof. Mark Allie and Prof. Eric Hoffman for their assistance with circuit and PCB design for the Tags. This work was supported by the National Science Foundation under grants CNS-2142978, CNS-2504963, CNS-2213688, and CNS-2112562.

References

[1] Advexure. 2023. RTK & Drones: A Comprehensive Guide to Centimeter-Level Accuracy. https://advexure.com/blogs/news/rtk-amp-drones-a-comprehensive-guide-to-centimeter-level-accuracy. Accessed: 2025-07-16.

[2] Sachin Agrawal, Sunil Kumar Pandey, Jawar Singh, and Manoj S. Parihar. 2014. Realization of efficient RF energy harvesting circuits employing different matching technique. In *Fifteenth International Symposium on Quality Electronic Design*. 754–761. https://doi.org/10.1109/ISQED.2014.6783403

[3] Aigen. 2025. Sustainable robotics for regenerative agriculture. https://www.aigen.io. Accessed: 2025-05-01.

[4] Charles K Alexander and Matthew N. O. Sadiku. 2017. *Fundamentals of electric circuits*. McGraw-hill Education New York, NY.

[5] Mohammad N Almasri and Jagath J Kaluarachchi. 2004. Assessment and management of long-term nitrate pollution of ground water in agriculture-dominated watersheds. *Journal of Hydrology* 295, 1 (2004), 225–245. https://doi.org/10.1016/j.jhydrol.2004.03.013

[6] M. Pareja Aparicio, A. Bakkali, J. Pelegri-Sebastia, T. Sogorb, V. Llario, and A. Bou. 2016. Radio Frequency Energy Harvesting - Sources and Techniques. In *Renewable Energy*, Wenping Cao and Yihua Hu (Eds.). IntechOpen, Rijeka, Chapter 7. https://doi.org/10.5772/61722

[7] FarmDroid ApS. 2025. The world's first fully automatic robot for sowing and mechanical weeding. https://www.farmdroid.dk. Accessed: 2025-05-01.

[8] Angelo Basile, Guido Ciollaro, and Antonio Coppola. 2003. Hysteresis in soil water characteristics as a key to interpreting comparisons of laboratory and field measured hydraulic properties. *Water Resources Research* 39, 12 (2003).

[9] Bernhard Bauer-Marschallinger, Vahid Freeman, Senmao Cao, Christoph Paulik, Stefan Schaufler, Tobias Stachl, Sara Modanesi, Christian Massari, Luca Ciabatta, Luca Brocca, et al. 2018. Toward global soil moisture monitoring with Sentinel-1: Harnessing assets and overcoming obstacles. *IEEE Transactions on Geoscience and Remote Sensing* 57, 1 (2018), 520–539.

[10] Zhaoxin Chang, Fusang Zhang, Jie Xiong, Junqi Ma, Beihong Jin, and Daqing Zhang. 2022. Sensor-Free Soil Moisture Sensing Using LoRa Signals. *Proc. ACM Interact. Mob. Wearable Ubiquitous Technol.* 6, 2, Article 45 (jul 2022), 27 pages. https://doi.org/10.1145/3534608

[11] Qasim Chaudhari. 2020. Carrier Phase-Based Ranging in Indoor Multipath Channels. *Wireless Pi* (2020). https://wirelesspi.com/carrier-phase-based-ranging-in-indoor-multipath-channels/

[12] Baicheng Chen, John Nolan, Xinyu Zhang, and Wan Du. 2024. MetaSoil: Passive mmWave Metamaterial Multi-layer Soil Moisture Sensing. In *Proceedings of the 22nd ACM Conference on Embedded Networked Sensor Systems (SenSys)*. ACM. https://doi.org/10.1145/3666025.3699334

[13] EA Colman. 1946. The place of electrical soil-moisture meters in hydrologic research. *Eos, Transactions American Geophysical Union* 27, 6 (1946), 847–853.

[14] ConnectedCrops. Accessed: 2024. A Guide to Soil Moisture. https://connectedcrops.ca/the-ultimate-guide-to-soil-moisture/.

[15] Dybowski D, Dzierzbicka-Glowacka LA, Pietrzak S, Juszkowska D, and Puszkarczuk T. 2020. Estimation of nitrogen leaching load from agricultural fields in the Puck Commune with an interactive calculator. *PeerJ* (2020).

[16] Department of ECology, State of Washington. 2023. *Reservoir Staff Gauge Guidance*.

[17] Advanced Linear Devices. Accessed: 2023. ALD Dual N-Channel MOSFET Array. https://www.aldinc.com/pdf/ALD110802.pdf.

[18] DFRobot. 2024. Gravity: Analog Capacitive Soil Moisture Sensor - Corrosion Resistant. https://store-usa.arduino.cc/products/gravity-analog-capacitive-soil-moisture-sensor-corrosion-resistant. Accessed: 2024.
[19] Jian Ding and Ranveer Chandra. 2018. *Estimating Soil Moisture and Electrical Conductivity Using Wi-Fi.* Technical Report. Microsoft Research. https://www.microsoft.com/en-us/research/wp-content/uploads/2018/10/SMURF_TR-1.pdf
[20] Jian Ding and Ranveer Chandra. 2019. Towards low cost soil sensing using Wi-Fi. In *The 25th Annual International Conference on Mobile Computing and Networking (MobiCom'19)*. 1–16.
[21] Rong Ding, Haiming Jin, Dong Xiang, Xiaocheng Wang, Yongkui Zhang, Dingman Shen, Lu Su, Wentian Hao, Mingyuan Tao, Xinbing Wang, and Chenghu Zhou. 2023. Soil Moisture Sensing with UAV-Mounted IR-UWB Radar and Deep Learning. *Proc. ACM Interact. Mob. Wearable Ubiquitous Technol.* 7, 1, Article 11 (March 2023), 25 pages. https://doi.org/10.1145/3580867
[22] Koffi Djaman, Komlan Koudahe, Aminou Saibou, Murali Darapuneni, Charles Higgins, and Suat Irmak. 2022. Soil Water Dynamics, Effective Rooting Zone, and Evapotranspiration of Sprinkler Irrigated Potato in a Sandy Loam Soil. *Agronomy* 12, 4 (2022). https://doi.org/10.3390/agronomy12040864
[23] Myron C Dobson, Fawwaz T Ulaby, Martti T Hallikainen, and Mohamed A El-Rayes. 1985. Microwave dielectric behavior of wet soil-Part II: Dielectric mixing models. *IEEE Transactions on geoscience and remote sensing* 1 (1985), 35–46.
[24] Inc. EarthSense. 2025. TerraSentia autonomous phenotyping robot. https://www.earthsense.co. Accessed: 2025-05-01.
[25] SparkFun Electronics. 2024. SparkFun Soil Moisture Sensor. https://www.sparkfun.com/products/13322. Accessed: 2024.
[26] Dara Entekhabi, Eni G Njoku, Peggy E O'neill, Kent H Kellogg, Wade T Crow, Wendy N Edelstein, Jared K Entin, Shawn D Goodman, Thomas J Jackson, Joel Johnson, et al. 2010. The soil moisture active passive (SMAP) mission. *Proc. IEEE* 98, 5 (2010), 704–716.
[27] Pasternack Enterprises. 2024. Friis Transmission Equation. https://www.pasternack.com/t-calculator-friis.aspx. Accessed: July 2024.
[28] Cornell University Cooperative Extension. Accessed: 2025. Soil Hydrology AEM. https://nrcca.cals.cornell.edu/soil/CA2/CA0212.1-3.php.
[29] Yuda Feng, Yaxiong Xie, Deepak Ganesan, and Jie Xiong. 2022. LTE-Based Low-Cost and Low-Power Soil Moisture Sensing. In *Proceedings of the 20th ACM Conference on Embedded Networked Sensor Systems (SenSys'22)*. 421–434.
[30] Daniel K. Fisher, Lisa K. Woodruff, Saseendran S. Anapalli, and Srinavasa R. Pinnamaneni. 2018. Open-Source Wireless Cloud-Connected Agricultural Sensor Network. *Journal of Sensor and Actuator Networks* 7, 4 (2018). https://doi.org/10.3390/jsan7040047
[31] GeoNadir. 2023. RTK Explained: What it is and why it matters. https://geonadir.com/rtk-explained/. Accessed: 2025-07-16.
[32] Manash Protim Goswami, Babak Montazer, and Utpal Sarma. 2018. Design and characterization of a fringing field capacitive soil moisture sensor. *IEEE transactions on instrumentation and measurement* 68, 3 (2018), 913–922.
[33] Meter Group. 2023. TEROS 12 Advanced Soil Moisture Sensor + Temperature and EC. https://metergroup.com/products/teros-12/.
[34] Daniel Hillel. 2013. *Introduction to soil physics.* Academic press.
[35] Agbotiname Imoize and A.I. Oseni. 2019. Investigation and pathloss modeling of fourth generation long term evolution network along major highways in Lagos Nigeria. *Ife Journal of Science* 21 (04 2019), 39. https://doi.org/10.4314/ijs.v21i1.4
[36] Campbell Scientific Inc. 2001. Soil water status: content and potential. *Campbell Scientific, Inc. App. Note: 2S-1* (2001). http://s.campbellsci.com/documents/ca/technical-papers/soilh20c.pdf
[37] Skyworks Solutions Inc. 2023. SMS7630 Schottky Diodes. https://www.skyworksinc.com/Products/Diodes/SMS7630-Series.
[38] Texas Instruments. 2025. TI CC1125 datasheet. http://www.ti.com/lit/ds/symlink/cc1125.pdf.
[39] Richard C. Jaeger and Travis N. Blalock. 2016. *Microelectronic circuit design.* McGraw-hill Education New York, NY.
[40] Chaowanan Jamroen, Preecha Komkum, Chanon Fongkerd, and Wipa Krongpha. 2020. An Intelligent Irrigation Scheduling System Using Low-Cost Wireless Sensor Network Toward Sustainable and Precision Agriculture. *IEEE Access* 8 (2020), 172756–172769. https://api.semanticscholar.org/CorpusID:222095629
[41] Wenli Jiao, Ju Wang, Yelu He, Xiangdong Xi, and Fuwei Wang. 2023. SoilTAG: Fine-Grained Soil Moisture Sensing Through Chipless Tags. *IEEE Transactions on Mobile Computing* (2023).
[42] Laney K Johnson A. 2021. Reducing the Health Impacts of the Nitrogen Problem. National Academies of Sciences, Engineering, and Medicine, Washington, DC, USA. https://doi.org/10.17226/26328
[43] Colleen Josephson, Manikanta Kotaru, Keith Winstein, Sachin Katti, and Ranveer Chandra. 2021. Low-Cost In-Ground Soil Moisture Sensing with Radar Backscatter Tags. In *ACM SIGCAS Conference on Computing and Sustainable Societies* (Virtual Event, Australia) *(COMPASS'21)*. Association for Computing Machinery, New York, NY, USA, 299–311. https://doi.org/10.1145/3460112.3472326
[44] Samar Kaddouri, Marwan El Hajj, Gheorghe Zaharia, and Ghais El Zein. 2018. Indoor Path Loss Measurements and Modeling in an Open-Space Office at 2.4 GHz and 5.8 GHz in the Presence of People. In *2018 IEEE 29th Annual International Symposium on Personal, Indoor and Mobile Radio Communications (PIMRC)*. 1–7. https://doi.org/10.1109/PIMRC.2018.8580695
[45] Usman Mahmood Khan and Muhammad Shahzad. 2022. Estimating Soil Moisture Using RF Signals. In *Proceedings of the 28th Annual International Conference on Mobile Computing And Networking* (Sydney, NSW, Australia) *(MobiCom'22)*. Association for Computing Machinery, New York, NY, USA, 242–254. https://doi.org/10.1145/3495243.3517025
[46] Yongcheol Kim, R.G. Evans, and W.M. Iversen. 2008. Remote sensing and control of an irrigation system using a distributed wireless sensor network. *IEEE Transactions on Instrumentation and Measurement* 57, 7 (2008), 1379–1387. https://doi.org/10.1109/TIM.2008.917198

[47] Daniel Kiv, Garvita Allabadi, Berkay Kaplan, and Robin Kravets. 2022. smol: Sensing Soil Moisture using LoRa. In *Proceedings of the 1st ACM Workshop on No Power and Low Power Internet-of-Things*. 21–27.

[48] Anja Klotzsche, François Jonard, Majken Caroline Looms, Jan van der Kruk, and Johan A Huisman. 2018. Measuring soil water content with ground penetrating radar: A decade of progress. *Vadose Zone Journal* 17, 1 (2018), 1–9.

[49] Mamta Kurvey and Ashwini Kunte. 2018. RF Energy Harvesting System. In *2018 International Conference on Smart City and Emerging Technology (ICSCET)*. 1–4. https://doi.org/10.1109/ICSCET.2018.8537306

[50] Lime Microsystems. 2017. LimeSDR Mini. https://www.crowdsupply.com/lime-micro/limesdr-mini. Accessed: July 22, 2025.

[51] Linx Technologies. Accessed: July 30, 2025. ANT-916-CW-RCS. https://www.digikey.com/en/products/detail/te-connectivity-linx/ANT-916-CW-RCS/340139.

[52] Wei Liu, Xiangyun Zhou, Salman Durrani, Hani Mehrpouyan, and Steven D Blostein. 2015. Energy Harvesting Wireless Sensor Networks: Delay Analysis Considering Energy Costs of Sensing and Transmission. arXiv:1509.06089 [cs.IT] Available at https://arxiv.org/abs/1509.06089.

[53] Zhehao Liu, Weizhi Wang, Swarun Gupta, and Vivek Iyer. 2024. ISAC: From Human to Environmental Sensing. *arXiv preprint arXiv:2507.13766* (2024). Available at https://arxiv.org/abs/2507.13766.

[54] Mohammed Bahjat Majed, Rahman, Tharek Abd, Omar Abdul Aziz, Mohammad Nour Hindia, and Effariza Hanafi. 2018. Channel Characterization and Path Loss Modeling in Indoor Environment at 4.5, 28, and 38GHz for 5G Cellular Networks. *International Journal of Antennas and Propagation* (2018).

[55] Blake R Marshall, Marcin M Morys, and Gregory D Durgin. 2015. Parametric analysis and design guidelines of RF-to-DC Dickson charge pumps for RFID energy harvesting. In *2015 IEEE International Conference on RFID (RFID)*. IEEE, 32–39.

[56] J. Martínez-Fernández, A. González-Zamora, N. Sánchez, A. Gumuzzio, and C.M. Herrero-Jiménez. 2016. Satellite soil moisture for agricultural drought monitoring: Assessment of the SMOS derived Soil Water Deficit Index. *Remote Sensing of Environment* 177 (2016), 277–286. https://doi.org/10.1016/j.rse.2016.02.064

[57] James Millerd, Neal Brock, John Hayes, Brad Kimbrough, Matt Novak, Michael North-Morris, and James C. Wyant. 2005. Modern approaches in phase measuring metrology. In *Optical Measurement Systems for Industrial Inspection IV*, Vol. 5856. SPIE, 1–12. https://doi.org/10.1117/12.621581

[58] J. Miranda, R. Abrishambaf, T. Gomes, P. Gonçalves, J. Cabral, A. Tavares, and J. Monteiro. 2013. Path loss exponent analysis in Wireless Sensor Networks: Experimental evaluation. In *2013 11th IEEE International Conference on Industrial Informatics (INDIN)*. 54–58. https://doi.org/10.1109/INDIN.2013.6622857

[59] Deepak Mishra, Swades De, and Kaushik Chowdhury. 2015. Charging Time Characterization for Wireless RF Energy Transfer. *IEEE Transactions on Circuits and Systems II: Express Briefs* 62 (04 2015), 1–1. https://doi.org/10.1109/TCSII.2014.2387732

[60] Surajo Muhammad, Jun Jiat Tiang, Sew Kin Wong, Ali H. Rambe, Ismahayati Adam, Amor Smida, Mohamed Ibrahim Waly, Amjad Iqbal, Adamu Saidu Abubakar, and Mohd Najib Mohd Yasin. 2022. Harvesting Systems for RF Energy: Trends, Challenges, Techniques, and Tradeoffs. *Electronics* 11, 6 (2022). https://doi.org/10.3390/electronics11060959

[61] Masaki Muramatsu and Hirotaka Koizumi. 2010. An experimental result using RF energy harvesting circuit with Dickson charge pump. In *2010 IEEE International Conference on Sustainable Energy Technologies (ICSET)*. IEEE, 1–4.

[62] Nuand. Accessed: 2024. BladeRF - Full-duplex software-defined radio. https://www.nuand.com/bladerf-1/.

[63] University of Minnesota Extension. Accessed: 2025. Soil Moisture Sensors for Irrigation Scheduling. https://extension.umn.edu/irrigation/soil-moisture-sensors-irrigation-scheduling.

[64] Ugur Olgun, Chi-Chih Chen, and John L. Volakis. 2011. Investigation of Rectenna Array Configurations for Enhanced RF Power Harvesting. *IEEE Antennas and Wireless Propagation Letters* 10 (2011), 262–265. https://doi.org/10.1109/LAWP.2011.2136371

[65] V. Pandey and P. Pandey. 2010. Spatial and Temporal Variability of Soil Moisture. *International Journal of Geosciences* (2010), 87–98. https://doi.org/10.4236/ijg.2010.12012.

[66] Polycase Inc. Accessed: July 2025. Water Proof IP Rated Boxes. https://www.polycase.com/ip-rated-enclosures.

[67] Ettus Research. Accessed: 2023. Ettus Research USRPB210. https://www.ettus.com/all-products/ub210-kit/.

[68] LA Richards. 1942. Soil moisture tensiometer materials and construction. *Soil Science* 53, 4 (1942), 241–248.

[69] Yaman Sangar, Yoganand Biradavolu, Kai Pederson, Vaishnavi Ranganathan, and Bhuvana Krishnaswamy. 2023. PACT: Scalable, Long-Range Communication for Monitoring and Tracking Systems Using Battery-less Tags. *Proc. ACM Interact. Mob. Wearable Ubiquitous Technol.* 6, 4, Article 180 (jan 2023), 27 pages. https://doi.org/10.1145/3569471

[70] Adel S. Sedra, Kenneth C. Smith, Tony Chan Carusone, and Vincent Gaudet. 2020. *Microelectronic Circuits* (8th ed.). Oxford University Press.

[71] Skyworks Solutions Inc. 2023. SKY66298-11 900-990 MHz Power Amplifier Datasheet. https://www.mouser.com/datasheet/2/472/SKY66298_11_204756_PS-1620853.pdf. Accessed: 2024-04-30.

[72] K. C. A. Smith and R. E. Alley. 1992. *Bibliography*. Cambridge University Press, 566–566.

[73] STMicroelectronics. 2022. S2-LP: Ultra-low power, high performance, sub-1GHz RF transceiver. https://www.st.com/en/wireless-transceivers/s2-lp.html. Accessed: 2024-04-30.

[74] STMicroelectronics. 2022. STEVAL-FKI868V2: S2-LP 868 MHz development kit with STM32L and USB interface. https://www.st.com/en/evaluation-tools/steval-fki868v2.html. Accessed: 2024-04-30.
[75] STMicroelectronics. 2022. STM32L053R8: Ultra-low-power 32-bit MCU with 64 KB Flash, 32 MHz CPU, LCD, USB, ADC, DAC and comparators. https://www.st.com/en/microcontrollers-microprocessors/stm32l053r8.html. Accessed: 2024-04-30.
[76] Texas Instruments. 2023. TPS22917 Load Switch Datasheet. https://www.ti.com/lit/gpn/tps22917. Accessed: 2024-04-30.
[77] Texas Instruments. Accessed: July 30, 2025. CC1310. https://www.ti.com/product/CC1310.
[78] GC Topp, M Yanuka, WD Zebchuk, and S Zegelin. 1988. Determination of electrical conductivity using time domain reflectometry: Soil and water experiments in coaxial lines. *Water Resources Research* 24, 7 (1988), 945–952.
[79] G Clarke Topp, JL Davis, and Aa P Annan. 1980. Electromagnetic determination of soil water content: Measurements in coaxial transmission lines. *Water resources research* 16, 3 (1980), 574–582.
[80] Le-Giang Tran, Hyouk-Kyu Cha, and Woo-Tae Park. 2017. RF power harvesting: a review on designing methodologies and applications. *Micro and Nano Systems Letters* (2017). https://doi.org/10.1186/s40486-017-0051-0
[81] Fawwaz T Ulaby and David G Long. 2014. *Microwave Radar and Radiometric Remote Sensing*. University of Michigan Press.
[82] Fawwaz Tayssir Ulaby and Umberto Ravaioli. 2015. *Fundamentals of applied electromagnetics*. Vol. 7. Pearson Upper Saddle River, NJ.
[83] Natural Resources Conservation Service United States Department of Agriculture. 1997. National Engineering Handbook, Part 652, Irrigation Guide: Chapter 3 – Soil–Plant–Water Relationships. https://efotg.sc.egov.usda.gov/references/public/FL/Nehfl652ch_3.pdf. Accessed: 2025-09-22.
[84] United States Department of Agriculture, Natural Resources Conservation Service. 2024. Web Soil Survey. https://websoilsurvey.sc.egov.usda.gov. Accessed: July 2025.
[85] Christopher R. Valenta and Gregory D. Durgin. 2014. Harvesting Wireless Power: Survey of Energy-Harvester Conversion Efficiency in Far-Field, Wireless Power Transfer Systems. *IEEE Microwave Magazine* 15, 4 (2014), 108–120. https://doi.org/10.1109/MMM.2014.2309499
[86] Ju Wang, Liqiong Chang, Shourya Aggarwal, Omid Abari, and Srinivasan Keshav. 2020. Soil moisture sensing with commodity RFID systems. In *Proceedings of the 18th International Conference on Mobile Systems, Applications, and Services (MobiSys'20)*. 273–285.
[87] Juexing Wang, Yuda Feng, Gouree Kumbhar, Guangjing Wang, Qiben Yan, Qingxu Jin, Robert C Ferrier, Jie Xiong, and Tianxing Li. 2024. SoilCares: Towards Low-cost Soil Macronutrients and Moisture Monitoring Using RF-VNIR Sensing. In *Proceedings of the 22nd Annual International Conference on Mobile Systems, Applications and Services*. 196–209.
[88] Nengcheng Wang, Naiqian Zhang, and Maohua Wang. 2006. Wireless sensors in agriculture and food industry—Recent development and future perspective. *Computers and Electronics in Agriculture* 50, 1 (2006), 1–14. https://doi.org/10.1016/j.compag.2005.09.003
[89] Dianjun Zhang and Guoqing Zhou. 2016. Estimation of soil moisture from optical and thermal remote sensing: A review. *Sensors* 16, 8 (2016), 1308.

Appendix

A Primer on Soil Moisture Sensing

Soil moisture, the amount of water in soil, is usually measured by volumetric water content (VWC), defined as the ratio of water volume to soil volume. The most accurate method for measuring soil moisture is the gravimetric method, which involves taking a soil sample and weighing it before and after drying it in an oven. However, this approach is time-consuming, labor-intensive, and not suitable for real-time monitoring. Commercial soil moisture sensors provide instant, in-situ readings by sensing indirect properties that are closely correlated with soil moisture. A widely used property is soil dielectric permittivity (ϵ), a fundamental electrical property of a material, given as a complex value: $\epsilon = \epsilon' + j\epsilon''$, where ϵ' and ϵ'' denote the real and imaginary parts of ϵ, respectively. Dielectric-based soil sensors rely on the relative permittivity of soil, which is defined as the ratio of the soil's absolute permittivity to the permittivity of free space ϵ_0 (8.854×10^{-12} F/m). The relative permittivity is given by: $\epsilon_r = \epsilon/\epsilon_0 = \epsilon_r' + j\epsilon_r''$, where ϵ_r' and ϵ_r'' are the real and imaginary parts of ϵ_r, respectively.

The permittivity detected by soil sensors in situ is called the apparent permittivity ϵ_a, given as:

$$\epsilon_a = \frac{\epsilon_r'}{2}\left[\sqrt{1+\tan^2\delta}+1\right] \tag{6}$$

where $\tan\delta$ is the loss tangent, which determines how lossy a medium is. It is defined as a function of the soil's relative permittivity ϵ_r, electrical conductivity σ, and radio frequency f:

$$\tan\delta = \frac{\epsilon_r'' + \frac{\sigma}{2\pi f \epsilon_0}}{\epsilon_r'} \tag{7}$$

The apparent permittivity ϵ_a is often used to estimate soil moisture, i.e., volumetric water content (θ), through empirical models such as Topp's equation [79]. This widely used model relates soil moisture to apparent permittivity as follows:

$$\theta = -5.3 \times 10^{-2} + 2.92 \times 10^{-2}\epsilon_a - 5.5 \times 10^{-4}\epsilon_a^2 + 4.3 \times 10^{-6}\epsilon_a^4 \tag{8}$$

where the constants are empirically derived to fit the relationship between ϵ_a and θ. This equation can be applied by substituting the value of ϵ_a to calculate the volumetric water content θ of the soil.

Path Loss in Soil. Soil is a lossy medium that causes additional attenuation of wave propagation compared to that in air. The total path loss of waves propagating between a transmitter (Tx) and a receiver (Rx), both placed underground, is the sum of two types of losses, namely: (1) Transmission loss L_t (2) Spreading loss L_{ss}

Transmission loss occurs when a plane wave propagates through soil. It is captured by the impulse response of the wireless channel at frequency f, wavelength λ, over a distance d_s, traveling at the speed of light c, as:

$$h(f,d) = Ae^{-\gamma d_s} = Ae^{-(\alpha+j\beta)d_s} = Ae^{-\alpha d_s}e^{-j\beta d_s} \tag{9}$$

where A is the signal strength, and γ is the complex propagation constant of soil. γ consists of α, the attenuation coefficient that determines signal attenuation, and β, the phase coefficient that determines phase rotation. The coefficients α and β are themselves non-linear functions of soil permittivity and the wavelength λ_0.

$$\alpha = \frac{2\pi}{\lambda_0}\sqrt{\frac{\epsilon_r'}{2}\left[\sqrt{1+\tan^2\delta}-1\right]}, \beta = \frac{2\pi}{\lambda_0}\sqrt{\frac{\epsilon_r'}{2}\left[\sqrt{1+\tan^2\delta}+1\right]} \tag{10}$$

Given the propagation characteristics and the attenuation coefficient, the transmission loss due to the soil's attenuation effect can be modeled as:

$$L_t = e^{2\alpha d_s} \tag{11}$$

This models how the signal strength of a plane wave decays exponentially with the attenuation coefficient α, and distance d_s.

Spreading loss is observed when a spherical wave originates from a point source (e.g., a transmit antenna) and is given by the Friis equation. The following equation captures the spreading loss in air:

$$L_s = \frac{P_r}{P_t} = \frac{1}{G_t G_r}\left(\frac{4\pi d_{tr}}{\lambda_0}\right)^2 \tag{12}$$

where P_r and P_t are the received and transmitted power, G_t and G_r are the gains of the transmitter (Tx) and receiver (Rx), $\lambda_0 = f/c$ is the wavelength in air, and d_{tr} is the distance between Tx and Rx. When the same setup is placed in soil, the spreading loss is similar to that in air (Equation 12), except for the wavelength; that is, λ_0 is replaced with λ, where $\lambda = 2\pi/\beta$.

For low salinity soils, we have $\epsilon_r'' \ll \epsilon_r'$ [23] and $\beta \approx 2\pi f \epsilon_r'/c = 2\pi\epsilon_r'/\lambda_0$. Thus, the spreading loss, L_{ss}, when both TX and RX are in the soil, can be approximated

$$L_{ss} = \frac{1}{G_t G_r}\left(\frac{4\pi d_{tr}\epsilon_r'}{\lambda_0}\right)^2 \tag{13}$$

The total path loss of the waves propagating between the Tx and Rx placed in soil is the sum of the transmission loss and the spreading loss, i.e., $L_t + L_{ss}$.